DEPARTMENT OF COMMERCE
LUTHER H. HODGES, Secretary

WEATHER BUREAU
F. W. REICHELDERFER, Chief

MONTHLY WEATHER REVIEW

JAMES E. CASKEY, JR., Editor

Volume 89
Number 5

MAY 1961

Closed April 15, 1961
Issued May 15, 1961

NORMAL HEAT SOURCES AND SINKS IN THE LOWER TROPOSPHERE IN WINTER

PHILIP F. CLAPP

Extended Forecast Section, U.S. Weather Bureau, Washington, D.C.
[Manuscript received November 18, 1960; revised March 2, 1961]

ABSTRACT

A synthesis is made of several published studies of the normal heat budget of the lower troposphere over the Northern Hemisphere in winter. Charts of heat sources and sinks are presented, based on two independent methods, one using the thermodynamic energy equation and the other a heat-balance procedure. Although there are differences in important details, both methods indicate that the horizontal scale of heating is the same as that of the normal lower-tropospheric temperature field, but that the field of heating is almost 90° out of phase with that of temperature.

This result has an important bearing on the energy budget of the circulation. It is concluded that the heat-balance method is correct in indicating that there is a positive correlation between the normal temperature and heating fields. According to the energy transformation equations, this means that there is a positive transformation from heating to potential energy at the scale of the climatological long waves. This energy is directly available for maintaining these waves against friction.

It is hoped that this study will be of some use in the design of numerical general circulation experiments, and as a basis of comparison with data from meteorological satellites.

1. INTRODUCTION

Attempts have been made by many investigators over the past 25 to 30 years to obtain an accurate picture of the distribution of sources and sinks of thermal energy which are responsible for driving the atmospheric circulation. Recent progress in improving the speed and capacity of electronic computers has raised the possibility of solving this problem, at least in principle, by including in a complex general-circulation model all the physical processes associated with heating and cooling. However, aside from the fact that these physical processes are poorly understood, there remains the difficulty that even the enormous speed and capacity of present machines are unequal to the task of resolving all of the complexities in a reasonable length of time. Therefore, in order to include some estimate of the heating fields in general circulation experiments, it has been necessary to employ simplified heating functions based largely on hypotheses arising from the judgment and experience of individual authors, as well as on the degree of complexity of their models (Phillips [25], Smagorinsky (to be published), Mintz [20], Charney [7], Fjørtoft [9]).

It is of vital importance that these estimates, though crude, give a reasonably accurate picture of the magnitude and pattern of the heat sources and sinks, because, as will be suggested at the conclusion of this article, their location relative to the different branches and space-time scales of the circulation is of critical importance in determining the sources of energy for, and therefore the life cycle of, these wind systems. Thus, there is evidently a need for a reasonably accurate picture of at least the normal fields of heating and cooling in the atmosphere so that these can be used as a check against the proposed heating functions.

There is also some evidence that the fields of heating and

cooling are closely related to errors in current operational numerical circulation forecasts (Martin [19]). Therefore, a knowledge of how these fields are related to upper-level wave patterns should be of considerable practical assistance in routine forecasting.

Finally, it is desirable to provide a rational basis of comparison with the directly observed values of the global heat budget obtained from meteorological satellites.

For these three reasons the author was encouraged to attempt an up-to-date and, it is hoped, accurate synthesis of these older estimates of the normal heat sources and sinks in the lower troposphere over the Northern Hemisphere. Encouragement in this effort was provided through the recent publication of the results of two extensive studies on this subject (Staff Members, Academia Sinica [29], Budyko [5] [6]).

2. GENERAL PROCEDURE

The first step was to make a search of the literature to locate all published studies of heating and cooling covering as much of the Northern Hemisphere as possible. This task was rendered fairly simple because of the relatively small number of projects treating the subject on so vast a geographical scale. Despite this restriction, it is possible that some of the pertinent literature may have been overlooked. Furthermore, the reader is cautioned that the list of references at the end of this paper is not meant to be an exhaustive bibliography on the subject, but contains only the reports actually used in this project.

Next, the publications were divided into those in which the heating fields were determined using the thermodynamic energy equation, and those based on a heat-balance method. It was hoped in this way to obtain two independent estimates, thus providing an accuracy check. However, it was soon discovered that the final results of the two methods were not comparable, and, as will be discussed later, it was necessary to make a choice as to which gives the more reliable results.

After the pertinent reports for each of the two methods had been selected, the data were read from the published charts at each standard 10° intersection of latitude and longitude from the equator to 60° N., and converted to mean heating in the layer 1000 to 500 mb. expressed in c.g.s. units (cal. gm.$^{-1}$ sec.$^{-1}\times 10^{7}$). (It was found that not enough data were available north of 60° N. to obtain heating fields in the polar regions.) In only one case were original data tabulations used for extracting the needed information.

The effect of reading published charts, rather than copying data tabulations, is to decrease the magnitudes of the maxima and minima of heating.

It was found that there were available no more than two independent sources of information dealing with any one particular type of heating field. These were simply averaged together in constructing the final charts, with no attempt to weight them in accordance with their probable relative accuracy. To a certain extent such a screening for accuracy was taken care of in the original careful selection of source material.

In some cases, only one source of data was available; and in one case, none at all. Thus, some reworking and extension of the original data was inevitable in order to obtain complete hemispheric heating fields. It must be stated that this was done in some instances by the use of approximate techniques which would probably not have been deemed entirely valid by the original authors. These modifications will be discussed in some detail below.

The general forms of the equations used in the computations are presented in Sections 3 and 4. These will not be derived here, as this has been taken care of in some detail in the original source references. However, the major assumptions on which they are based, and the additional approximations used by the individual authors, will be treated here.

The final heating fields presented in figures 1 to 5 may be considered to apply to the colder season and are averages for the layer 1,000 to 500 mb. or 0 to 5.5 km. No distinction was made between individual data fields for winter (December, January, and February), and those for the month of January only. Examination of normal flow patterns shows that there are relatively small changes in the principal meteorological parameters (and presumably also in the heating field) between the months of December and February.

3. THERMODYNAMIC ENERGY EQUATION METHOD

From the first law of thermodynamics and the definition of potential temperature, the individual rate of heating per unit mass, averaged over a specified time interval, may be written as follows:

$$\overline{\frac{dq}{dt}}=c_p\frac{\partial\overline{T}}{\partial t}+c_p\overline{\mathbf{V}}\cdot\nabla\overline{T}+\frac{c_pT}{\theta}\overline{w}\frac{\partial\overline{\theta}}{\partial z}+c_p\overline{\mathbf{V}'\cdot\nabla T'}+\frac{c_pT}{\theta}\overline{w'\frac{\partial\theta'}{\partial z}}. \tag{1}$$

Here, q is the amount of heat per unit mass; c_p, specific heat at constant pressure; T, absolute temperature; t, time; $\mathbf{V}$, horizontal wind vector; ∇, horizontal gradient; θ, potential temperature; w, vertical wind component; and z, height. The bar overscore represents the arithmetic-averaged value of a given quantity for the selected time interval, and the prime symbol denotes the departure of a quantity from its time-averaged value.

The terms on the right of equation (1) may be designated, in order, the local heating (heat storage term), horizontal heating (horizontal advection of heat), vertical heating (vertical advection of heat), horizontal eddy-advection of heat, and vertical eddy-advection of heat.

The two principal assumptions made in deriving equation (1) are relatively minor. They are: (a) The local rate-of-change and horizontal advection of pressure are

small compared to its vertical advection. (b) The quantity T/θ may be considered constant in time when used as a coefficient of the vertical heating term.

The first attempt to compute average heating from equation (1) was made by Wexler [31]. The results reported on here are based on the more recent studies of Aubert and Winston [2] and Staff Members, Academia Sinica [29], who computed the normal heating in the lower part of the troposphere for individual months or seasons of the year. Both of these studies omitted the two eddy terms and used a constant or normal vertical stability in evaluating $\partial\theta/\partial z$. They also used constant values of $\overline{\nabla}$, $\overline{T}$, and $\overline{w}$ within a finite vertical layer of the atmosphere. This is equivalent to assuming that there is no correlation in the vertical between the horizontal wind components and temperature, or between vertical motion and stability. Neither source made computations north of about 70° N. Few estimates were made by Aubert and Winston south of 20° N., and by Staff Members south of 10° N.

These two sources differ somewhat in other approximations used in their work as follows:

Aubert and Winston evaluated the heating for the layer sea level to 10,000 feet using normal sea level and 10,000-ft. charts. The gradient wind obtained from the average pressure field for this layer was used in computing $\overline{\nabla}$. The quantity $\overline{T}$ is the average mean virtual temperature between these two levels, and $\overline{w}$ was obtained from the divergence of the mean gradient winds. Their results must be questionable near high mountains, because pressures reduced to sea level were used, and no mountain-effect was included in the computation of $\overline{w}$.

The Staff Members used normal constant-pressure charts to evaluate heating in the layer 1,000 to 500 mb. (approximately sea level to 5.5 km.). The geostrophic wind at 700 mb. was used in computing $\overline{\nabla}$, and $\overline{T}$ was replaced by the thickness between the two layers. The mean vertical motion was obtained using the average divergence at the ground and at 500 mb. The authors state that the surface divergence was computed from observed winds, although it is difficult to see how this is possible in most areas of the globe, where no winds are available. The upper-level divergence was computed with the aid of the vertically integrated tendency equation. This seems to avoid the difficulty arising from the balance of terms in the divergence equation. The effect of topography was included in computing vertical motion at the ground, but this apparent improvement of the method of Aubert and Winston is largely nullified by the use of reduced 1000-mb. charts in computing thickness advection. Thus, their heating fields are probably also unreliable in mountain areas.

In order to obtain an average of these two heating fields, it was necessary to convert the values of mean heating in the layer 0 to 3 km., derived from data of Aubert and Winston, to the layer 0 to 5.5 km. This was done using the rather arbitrary assumption that the intensity of heating per unit mass varies linearly with height, reaching a maximum at 1 km. and vanishing at sea level and 10 km. Using this scheme, the ratio between average heating in the two layers can easily be obtained. Thus, the conversion was accomplished simply by dividing the values obtained from Aubert and Winston by 1.08.

The two independent estimates are remarkably similar (separate charts not shown). The major difference is in eastern Asia and the western Pacific, where the heating maximum computed by Staff Members is weaker and considerably farther to the east than that of Aubert and Winston. This discrepancy is difficult to trace, but may be due to the use of different normal circulation patterns.

The average of these two heating fields is shown in figure 1. A brief discussion of the pattern of heating and its relation to the broadscale temperature field will be deferred until Section 5. Here, an attempt will be made to assess its probable accuracy. This is not an easy matter, in view of the numerous assumptions discussed previously.

Inspection of figure 1 quickly reveals certain regions where one would suspect that the values are in error. For reasons given below, the indicated heating over eastern Canada and Siberia appears to be too large in comparison with that in the northwestern Atlantic and Pacific Oceans. Also, there is no apparent explanation for the small but positive heating over the oceans west of California and North Africa, which incidentally, appears on the charts of both authors. The northeastern continents and southeastern oceans in winter are known to be regions where precipitation is relatively light. This means that condensation, the only important source of heat in these areas, must be relatively weak. On the other hand, in both regions the air sometimes loses heat by contact with a colder land or ocean surface, and always loses heat by radiation to space.

Examination of the individual terms in equation (1) reveals the probable source of these errors. The reliability of the normal circulation patterns is probably quite acceptable, so that, except in the high mountain areas, the sum of the first two terms is reasonably correct. Thus the errors may be traced to the omission of the eddy terms and to the approximations used in computing vertical motion.

The necessity of accurate estimates of vertical motion stems from the fact that there is a strong negative correlation between the sum of the first two terms and the third term on the right side of equation (1). This has been demonstrated on a synoptic scale by Panofsky [24] who showed that vertical motions computed by the adiabatic method (essentially equation (1) with zero heating and the eddy terms omitted) are positively correlated with weather and with vertical motions computed from the divergence of observed winds (kinematic method). Several recent extensive studies of the kinetic energy

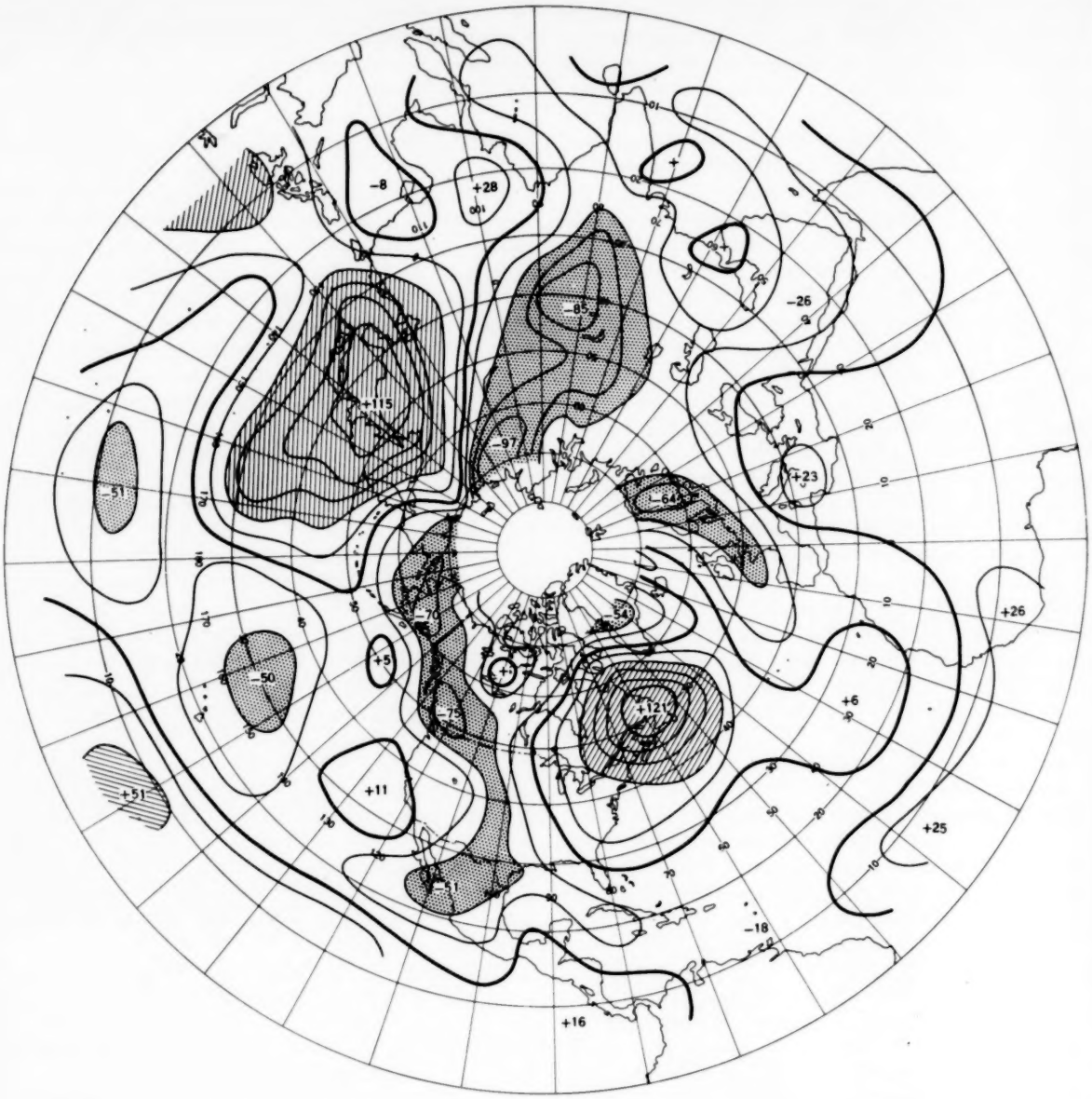

FIGURE 1.—Normal winter heating, sea level to 5.5 km., computed by the thermodynamic energy equation method. Units are cal. gm.$^{-1}$ sec.$^{-1}\times 10^{7}$. To convert to: cal. cm.$^{-2}$ day^{-1} multiply by 4; to C °. day^{-1}, by 4/100. Lines drawn for every 20 units with zero line heavier. Areas with heating greater than +40 units cross-hatched; cooling greater than −40 units stippled.

budget of the circulation have been based on vertical motions computed by the adiabatic method, evidently with some assurance that this gives reasonably accurate results, at least for that purpose (e.g., Jensen [15]).

Aubert and Winston [2] have shown that for nearly steady-state time-averaged circulations there is also a high negative correlation between the horizontal and vertical heating terms.

This tendency for a negative correlation between three of the important terms means that equation (1) must be used with extreme caution in estimating heating, since a large systematic error in any term may even lead to the wrong sign of the heating. This may result in serious errors in the spatial *pattern* as well as the *magnitude* of heating. This precaution applies especially to the term containing vertical motion, because all the known (indirect) methods of estimating the vertical wind component are subject to systematic errors.

In the two studies discussed here there is evidence that the computed vertical motions are too small. Indeed, Aubert and Winston show that for a few selected localities the mean monthly divergence (and therefore vertical motion) computed from observed winds is *four times* as large as the divergence of the gradient wind. This means that in general there is not enough compensation between the horizontal and the vertical terms. In regions of generally sinking motion in the northeastern continents and southeastern oceans this results in too much heating, while in the areas of slow mean upward motion in the western oceans, not enough heating is computed.

The omission of the eddy terms also has quite serious consequences in certain areas. Attempts to estimate the horizontal eddy effect (fourth term on the right of equation (1)) by an approximate theory of horizontal mixing have been made by Möller [21] and Elliott and Smith [8]. If it can be assumed that horizontal mixing is proportional to the horizontal temperature gradient, with a constant coefficient of proportionality, then it can be shown that:

$$\overline{\mathbf{V}' \cdot \nabla T'} = -A\nabla^2 \overline{T} \tag{2}$$

where A is called the "Austausch" coefficient (always positive according to theory), and $\nabla^2\overline{T}$ is the horizontal Laplacian of the mean temperature field (often called the thermal vorticity).

In regions of strong cyclonic thermal vorticity, as in the northeastern continental areas (see fig. 6), the eddy term is negative and, like the vertical motion term, tends to reduce the magnitude of heating given by the horizontal term alone. An opposite effect is produced in regions of anticyclonic thermal vorticity, as indicated by anticyclonic shear of the isotherms in the western oceans (fig. 6) and anticyclonic curvature in the northeastern oceans.

An attempt was made in the present study to include quantitative estimates of the eddy term as computed by equation (2), but this was abandoned in view of the obvious crudeness of this method as revealed by the studies of Möller and Elliott and Smith.

It is clear that the only way to avoid this problem completely is to compute the terms using synoptic maps and then average them over the desired time interval. This task, too laborious to accomplish on a large scale by the older "hand" methods, has recently been tackled with the aid of an electronic computer by Wiin-Nielsen and Brown (to be published). Their preliminary results for one winter month show that a region of weak cooling replaces the heating in figure 1 in eastern Canada. However, this may be due to the fact that the circulation for the chosen month (January 1959) was extremely abnormal at high latitudes.

The conclusions to be reached from the above arguments are that the strong heating centers in the northeastern continents in figure 1 should be weakened and shifted to the southeast, and that the weak heating in the southeastern oceans should be eliminated, or even replaced by centers of cooling.

4. HEAT-BALANCE METHOD

The sum of all sources of real heat gain or loss in a certain column of air of unit cross-section is equal to the flux-divergence plus the storage of heat in that column. With the aid of a continuity equation for real heat, it can be shown that the storage plus flux-divergence is equal to the total individual rate of heating. Thus, the average heating per unit mass in the column is given by the equation:

$$\overline{\frac{dq}{dt}} = \frac{g}{\Delta p}(\overline{Lr} + \overline{R} + \overline{P}). \tag{3}$$

Here g is the acceleration of gravity; Δp, the pressure difference between bottom and top of the column (here 500 mb.); Lr, the net heat gain due to condensation or evaporation; R, heating due to radiation; and P, that due to turbulent exchange with the earth's surface. As before, the bar overscore represents an average over a specified interval of time.

The only approximation in this equation is to omit other sources of heating or cooling which are generally considered negligible. Among these sources is the transformation between kinetic energy and heat in the frictional boundary layer.

As a matter of practical convenience, it is assumed in addition that (a) the net condensation and evaporation is measured by the heat equivalent of rain or snow reaching the ground; and (b) the radiation balance is determined by the net radiative inflow at the bottom and top of the column. In accordance with assumption (a) the quantity L in equation (3) is the latent heat of condensation or sublimation, and r is the amount of precipitation reaching the ground.

In practice the individual physical processes on the right of equation (3) are evaluated from climatological data. Thus, depending on the equations used, a certain residual effect is present, which is due to correlation in time between parameters appearing in these equations. The consequences of these "eddy" terms will be treated briefly in a later paragraph. Here it will only be stated that this is probably not very important.

In addition to being relatively free of errors associated with eddy terms, the heat-balance method has another important advantage over the thermodynamic energy equation method in that there is no tendency for compensation between individual terms, in the sense that there is a high negative pattern correlation between any two of them. In fact, just the opposite is true, as will be clarified in later paragraphs.

To compensate for these advantages, it is difficult to formulate the individual physical processes in mathematical terms. Even if this were possible, the necessary

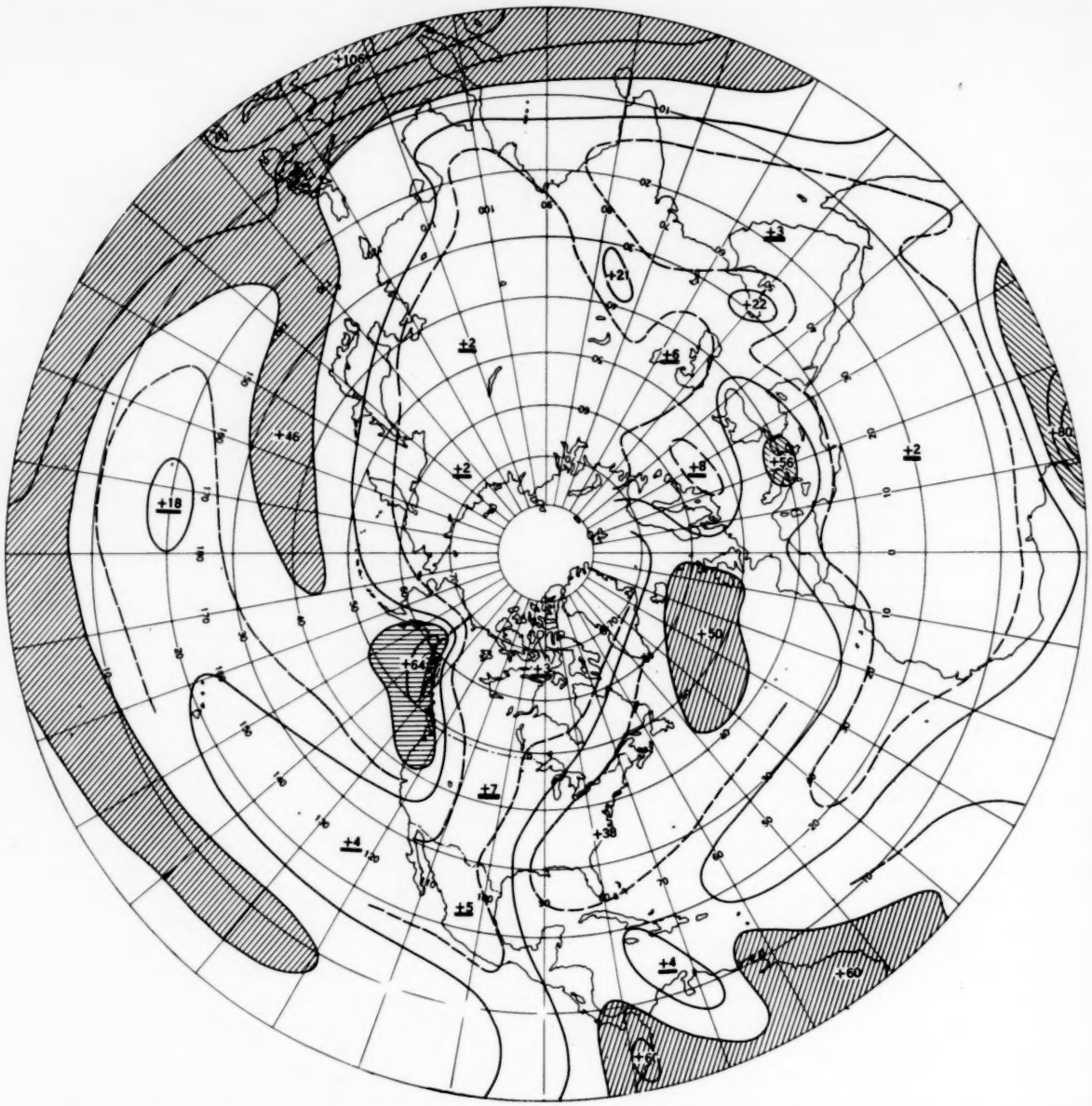

FIGURE 2.—Normal winter heating, sea level to 5.5 km. due to condensation and evaporation. See figure 1 for legend. Intermediate lines dashed, centers of relative minima underlined.

hemispheric data for evaluating them are frequently lacking.

A. EVAPORATION AND CONDENSATION

To evaluate this component of heating according to previous assumptions, it is necessary to determine the hemispheric distribution of winter precipitation, and simply convert this to heating units by multiplying it by the latent heat of condensation or sublimation. The result is then substituted for Lr in equation (3) under the assumption that all condensation takes place below the 500-mb. level.

Two separate fields were assembled, one using precipitation over the land by Landsberg [16] and over the oceans by Jacobs [14], and the second using hemispheric precipitation patterns worked up by Möller [22]. These were averaged and multiplied by a constant latent heat of condensation, equal to 600 cal. gm.$^{-1}$ The results are shown in figure 2. Strictly speaking the latent heat of sublimation should have been used in those areas where

precipitation reached the ground in the form of snow. In addition, the magnitude of latent heat should be a function of the temperature of condensation or sublimation. However, these refinements would make little difference in the magnitude and pattern of heating.

Another minor discrepancy arises from the assumption that the net condensation and evaporation is measured by precipitation reaching the ground. This is a good assumption except possibly in those areas where clouds form and drift into other regions before evaporating or discharging their moisture. However, the heat content of such clouds is probably quite small, and it is difficult to isolate large areas where a systematic effect of this kind is to be found.

More important than these considerations is the question of the accuracy of the precipitation amounts. Some encouragement is gained by noting that the two precipitation fields are very similar, both in pattern and magnitude (separate charts not shown). However, this must be tempered by the realization that the authors used similar procedures and sources of data.

Over the lands, precipitation amount is determined with fair reliability from direct observation.

Over the oceans, where direct observations are lacking, precipitation amount is determined from the frequency of rainfall. This is converted to precipitation by relating it to known amounts at island and coastal stations, after taking into account the effect of latitude and geographical location. The net result is to cast doubt on the magnitude, but not the pattern, of rainfall over ocean areas.

Two other sources of error influence the computed magnitude of heating, especially in the western oceans. The first is the truncation effect, mentioned earlier, due to reading precipitation charts at widely spaced grid points. This results in a reduction in the amplitude, or difference between maxima and minima. This is partly compensated by the second error, resulting from the fact that in regions of heavy rainfall cloud tops frequently extend above the 500-mb. level. Thus, part of the condensation occurs above the 1000- to 500-mb. layer, resulting in an overestimate of heating in these regions.

If the above conclusions are accurate, namely, that at least the *pattern* of heating shown in figure 2 is correct, this helps to establish the pattern of the *total* heat budget of the troposphere. For, as pointed out by Albrecht [1], and as will be shown further on in this report, there is a high positive correlation between the precipitation pattern and that of total heating.

B. SENSIBLE HEAT EXCHANGE

The gain or loss of real (sensible) heat by direct turbulent contact with the earth's surface was obtained for ocean areas from estimates by Jacobs [14] and Budyko [5]. Jacobs made use of the so-called "Bowen formula" which is based on an assumed simple ratio between the turbulent exchange of heat and that of water vapor. The evaporation is assumed to be given by the product of the wind at observation level times the vertical vapor-pressure gradient. The sensible heat exchange is thus a function of evaporation, temperature gradient, and water vapor gradient near the sea surface.

Budyko used a formula giving the heat exchange as the product of the wind and the vertical temperature gradient multiplied by a certain exchange coefficient which is assumed to be a constant.

These formulae are regarded by many authorities as being fairly reliable, in spite of the undeveloped state of boundary-layer turbulence theory. The exchange coefficient, assumed constant, is known to depend to some extent on stability. Normal winter values of the different parameters, determined with reasonable accuracy from ships' observations, were used in evaluating the equations.

The two separate heating patterns (not shown) are in good agreement, although it must be stated that essentially the same sources of oceanic data were used.

No winter charts of sensible heat exchange over land are known to the author. However, Budyko [5] presents a chart for the year as a whole, as well as values for each month of the year for 12 stations representing certain selected climatic zones. These values are obtained from the equation for heat balance of the land surface, expressing the sensible heat exchange as the difference between radiation of all wavelengths reaching the ground and the heat of evaporation. The amount of evaporation is in turn determined as the difference between total precipitation and runoff.

In order to obtain a rough estimate of the pattern of sensible heat exchange over land areas, the present author adopted the following scheme: (a) Using Köppen's climatic classifications, the land areas were subdivided into climatic zones approximating the definitions used by Budyko. (b) Within each zone, the difference between January heating and that for the year as a whole was assumed to be the same as that for the appropriate climatic station for that zone. (c) Budyko's yearly maps were then read at standard latitude-longitude intersections, and the results of step (b) applied to these yearly means. In order to read Budyko's maps, the lines of constant sensible heat exchange were extrapolated through mountainous areas although Budyko was careful to discontinue the lines in the higher elevations.

The results of this admittedly crude procedure are plotted in figure 3 along with the average of the two ocean estimates. Only the general magnitude and sign of the computations over land have any reliability. This shows, as one might expect, that the values are in general negative over northern continents (where relatively warm air flows over a cold snow surface) and positive over the southern continents (where cold air from the north flows over warmer snow-free ground), and that the largest magnitude (-16 units) is considerably smaller than those over the oceans. The general magnitude of heat loss over the northern continents is in fair agreement with independent estimates of others. For example, Hanson [12] has re-

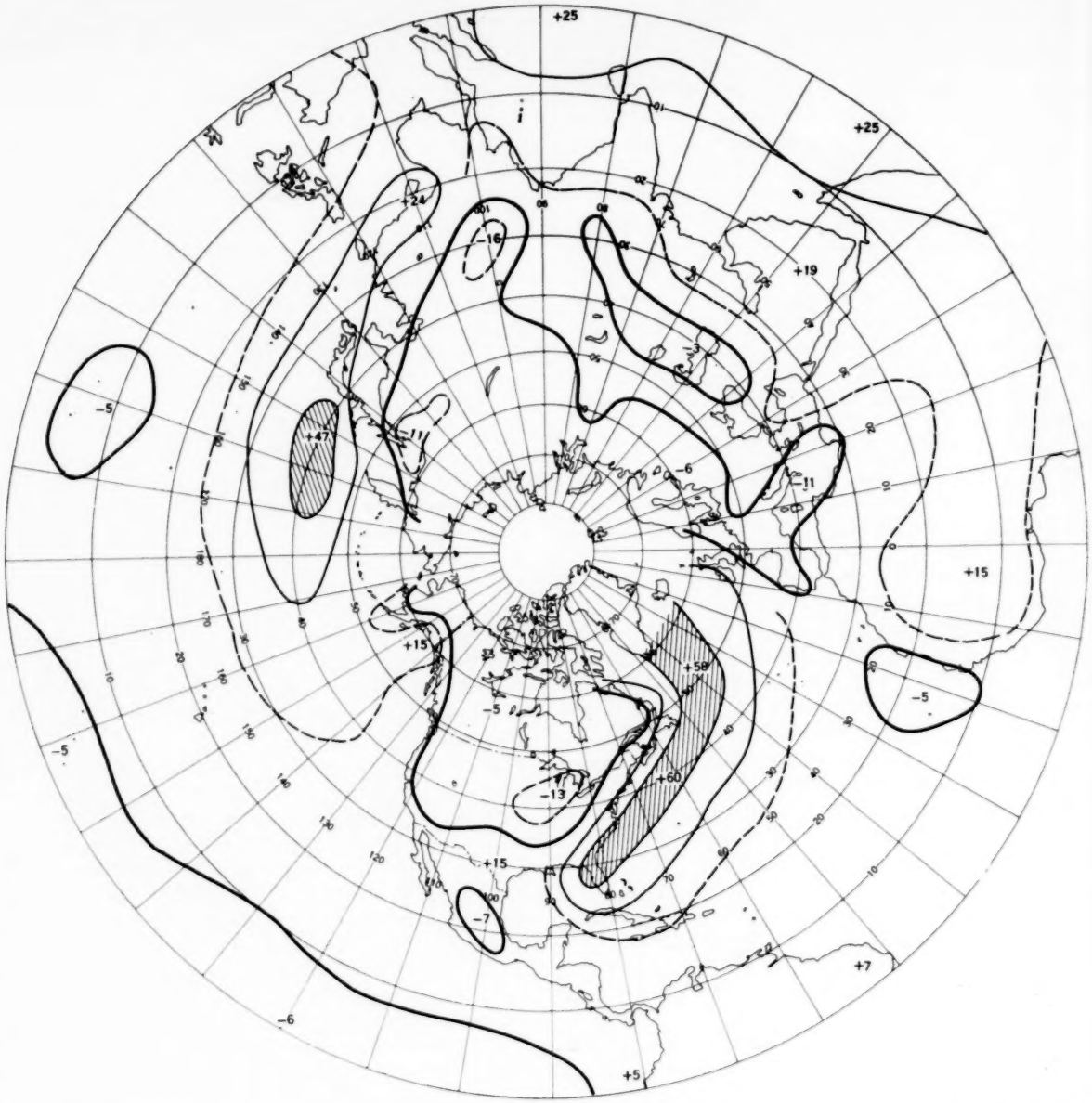

FIGURE 3.—Normal winter heating, sea level to 5.5 km. due to exchange of sensible heat with the earth's surface. See figure 1 for legend.

cently computed a value of −11 units at the South Pole in spring.

Comparison of figures 2 and 3 shows a high positive correlation between these two independent heating fields, as mentioned previously. This correlation is especially good north of 20° N.

C. THE RADIATION BALANCE

The third important component of the heat-balance is obtained by subtracting the net loss of radiation by all wavelengths at the bottom of the atmosphere from the net incoming radiation at the top. This radiation flux-divergence for the entire atmosphere is then "reduced" to the layer 1000–500 mb.

The net incoming radiation is obtained from Simpson's [28] classical computations, which appear to remain the only available source for the geographical distribution of this quantity. According to Godske et al. [11], Simpson's charts probably portray the pattern of radiation quite well, although recent advances in computation methods might well improve the magnitudes.

Simpson first computes the effective incoming short-wave solar radiation, and subtracts from this the net outgoing long-wave radiation. In his calculations, both of these quantities depend largely on cloudiness, latitude, and season. The outgoing long-wave radiation is obtained by Simpson's well-known technique of first dividing the black-body radiation curve into finite regions depending on the transparent or opaque parts of the water vapor spectrum. The outgoing radiation to space in the transparent regions depends on the normal surface temperature, while that in the opaque regions is assumed to depend on the temperature of the uppermost water vapor layer, located in the lower stratosphere. The temperature of the stratosphere is taken as a function of latitude only. When clouds are present, they are assumed to radiate as a black-body at constant temperature (260° A.). Simpson's method appears to result in too small values for the outgoing radiation, since later investigators have found that the effective upper water vapor layer lies well below the tropopause.

The net radiation loss of the air near the ground is taken from Budyko [5]*. This depends on a rather complicated chain of four empirical formulae of the type pioneered by Ångström and Brunt. The formulae depend on climatological mean values of albedo, cloud amount, the fourth power of surface air temperature, vapor pressure in the lower atmosphere, and the fraction of short-wave radiation reaching the ground with cloudy skies. The albedo depends on the latitude, season, and average type of ground cover; while the fraction of short-wave radiation reaching the ground with cloudy skies is assumed to be a function of latitude only.

In extracting data from Budyko's radiation maps the isolines were extended through mountain areas as in the case of the sensible heat. Also, after the results had been subtracted from Simpson's values and then analyzed, certain discontinuities depicted by Budyko along coastlines and the shores of inland water bodies were ignored.

This net radiative flux-divergence for the whole atmosphere was reduced to the layer 1000 to 500 mb. with the aid of London's [17] mean zonal cross-sections showing the local radiative heat loss as a function of altitude and latitude for each season. From London's cross-section for winter, a coefficient was obtained (for each latitude) equal to the ratio between the mean heating in the layer 1000–500 mb. and that for the entire layer 1000–0 mb. This was multiplied by the total flux-divergence for the appropriate latitude to obtain a reduced value. Finally, the latter was adjusted so that its zonal mean for each latitude agrees with those of London.

The final result of the various steps is shown in figure 4. Unlike the field of figure 3 the pattern correlates very poorly (although still slightly positively) with the net precipitation pattern shown in figure 2. It is easy to show qualitatively that this poor correlation is due largely to the method of reduction. This may be demonstrated with the aid of two schematic diagrams prepared by Möller [23] showing the variation with altitude of radiative flux-divergence with clear skies, and with cloudiness and rain. It is clear from these diagrams that in regions of small precipitation, where there are frequent clear skies or low clouds having tops well below the 500-mb. level, over half of the total radiative flux-divergence lies below 500 mb. Therefore in these regions (central and northern continents) the magnitude of radiative loss in the lower troposphere should be somewhat larger than that computed with a reduction factor depending on latitude alone. On the other hand, in regions of heavy precipitation, (western and northern oceans and near the equator) where cloud tops frequently reach to or above the 500-mb. level, the radiative flux-divergence shown in figure 4 must be sharply reduced because it is almost zero within and below the clouds. These modifications would clearly lead to an increase in the positive correlation between the fields of radiative heating and condensation.

No attempt has been made in this study to apply such modifications in a quantitative fashion. It was felt that this would be tantamount to "begging the question." The solution to this problem must await a fresh approach to the computation of radiative flux-divergence as a function of geography and elevation.

D. TOTAL HEATING

The sum of the three principal components of heat-balance is shown in figure 5. This is the final estimate of the normal heating of the lower troposphere by the heat-balance method. As expected, it shows a high positive pattern-correlation with the distribution of heating by precipitation (fig. 2) despite the unsatisfactory results for the radiative component (fig. 4). The lack of any major modification of the pattern is due to the fact that the radiation distribution is almost zonal, with relatively weak gradients. Correction of the field of radiation would have the effect of increasing the magnitude of the maxima and minima in figure 5 (especially the maxima) without changing the pattern greatly.

Albrecht [1] has computed the field of heating for the year as a whole, also using the heat-balance method. His pattern is quite similar to that in figure 5 over the oceans and along the eastern coasts of continents. As might be expected from seasonal changes in heating over land, his chart shows less cooling in continental interiors.

E. THE EDDY TERMS

It must be clear from the discussion in subsections A through D above that the most important question regarding the heat-balance method is that of the validity of the crude semi-empirical procedures used for evaluating the components. For this reason it seems almost beside the point to consider the possibility of additional errors due

*A similar study has been made by Bernhardt and Phillips [3]. Unfortunately, their complete radiative heat balance, including the long-wave components, was not available. However, it may be noted here that their charts of total short-wave radiation reaching the ground agree very well with those of Budyko.

588203—61——2

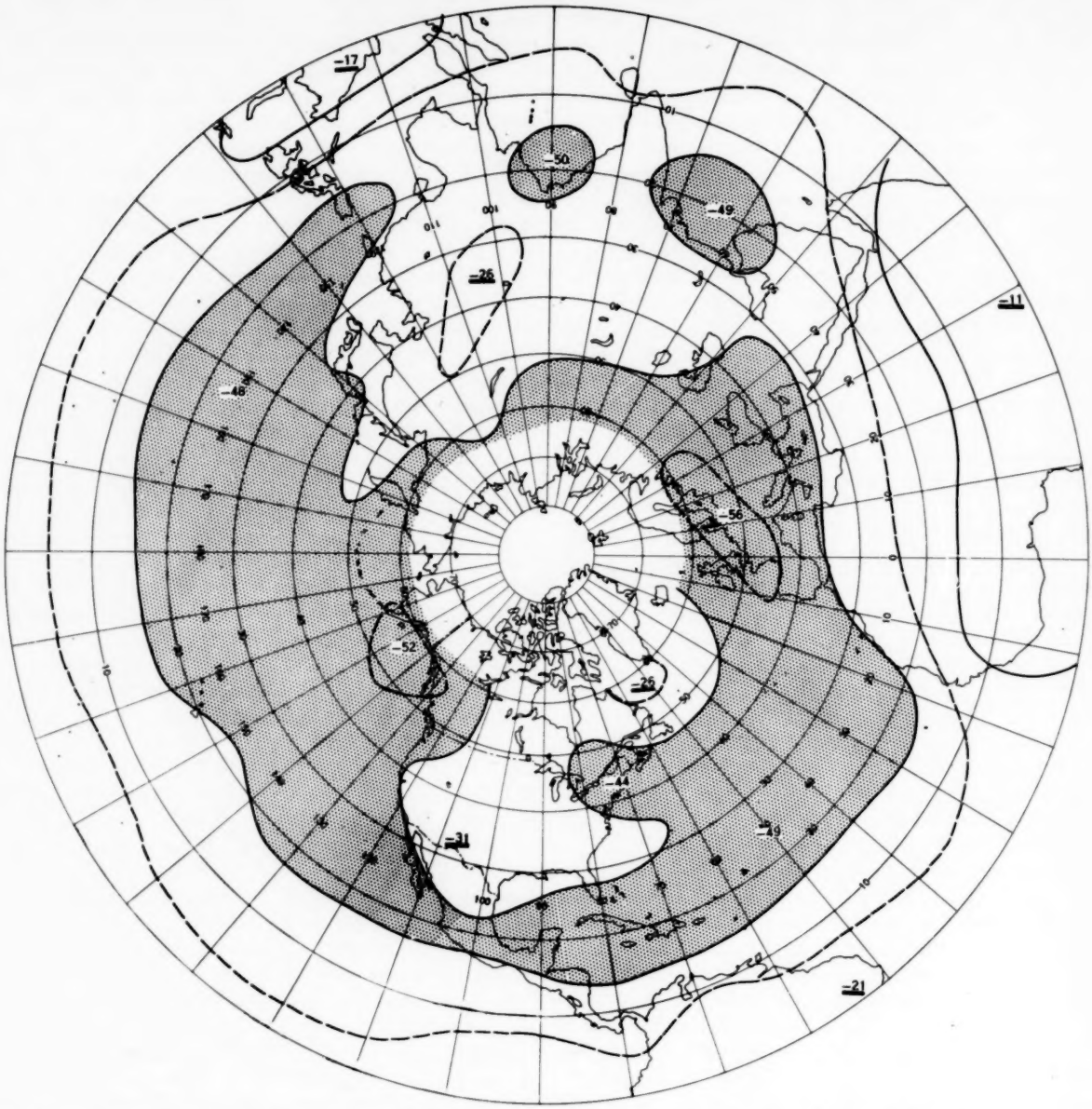

FIGURE 4.—Normal winter heating, sea level to 5.5 km. due to radiation of all wavelengths. See figure 1 for legend. Relative maxima underlined.

to correlation between the individual meteorological variables used in evaluating the equations. Furthermore the formulae for radiation and sensible heating have been designed specifically for use with climatic data, and would probably not be used if these two heating components were to be evaluated on a day-to-day basis. Nevertheless, the problem of eddy effects is so important for the thermodynamic energy equation method that it will also be raised in connection with the heat-balance method. Therefore, a brief discussion of its possible importance will be given here.

There is no eddy effect in the computation of heating by evaporation and condensation because this is obtained simply by summing the daily amounts or frequencies of precipitation. Therefore, it may be concluded that the pattern of precipitation (and presumably also the pattern of total heating) is free of errors from this effect.

The formula used by Budyko for sensible heat exchange

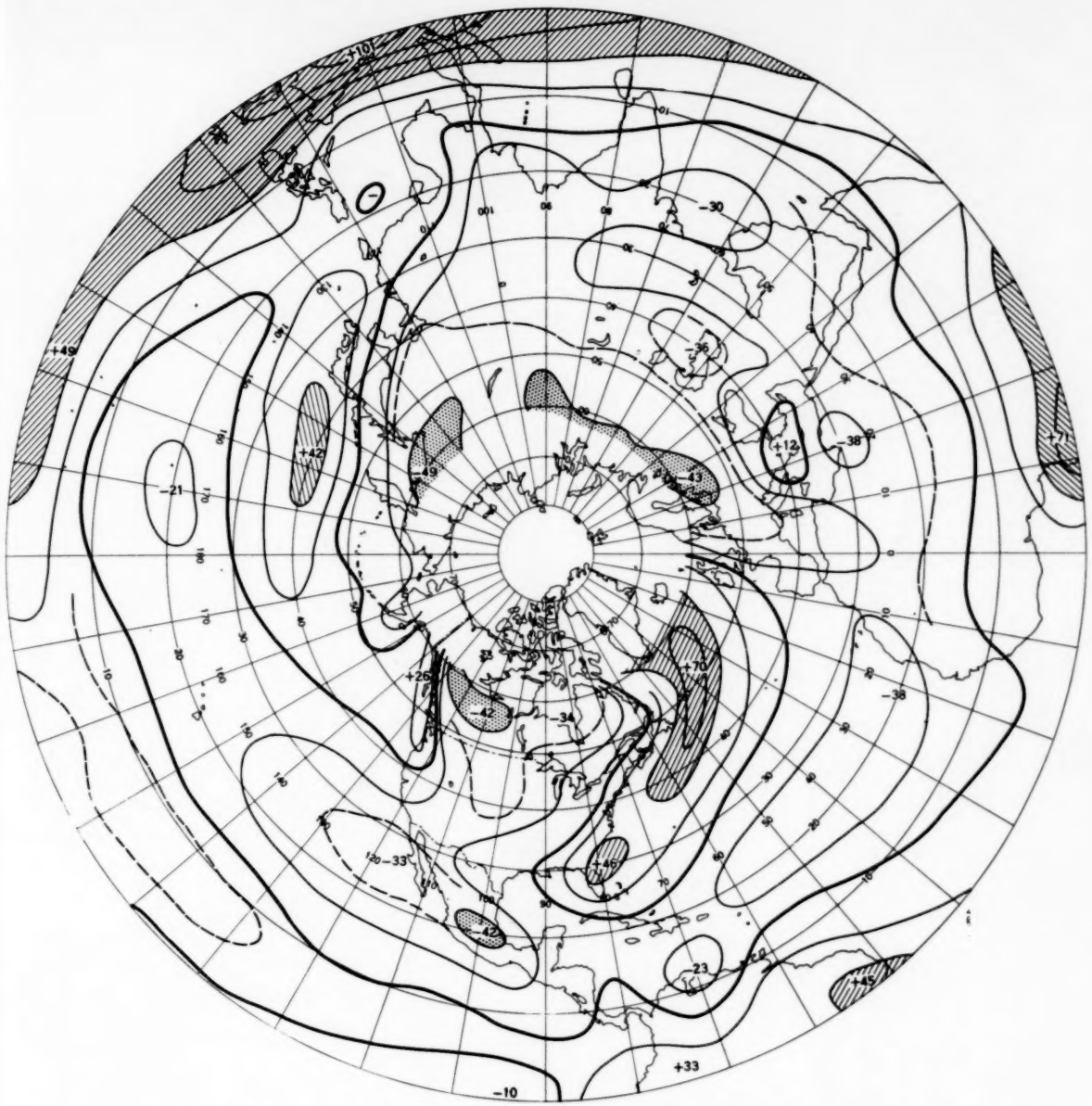

FIGURE 5.—Normal winter heating, sea level to 5.5 km., computed by the heat-balance method. See figure 1 for legend.

may be subject to some error due to a positive correlation between the exchange coefficient and the temperature gradient. This arises because the turbulence exchange coefficient becomes smaller the more stable is the lapse rate. This would lead to some increase in the estimate of heating over ocean areas portrayed in figure 3. However, Budyko [6] states that this effect is not important over oceans.

The crude estimates of this sensible heat component over land would fortunately not be further biased by eddy effects because the heating is estimated by linear heat-balance equations.

Since Jacobs used the Bowen ratio, the effect of a variable coefficient is partly eliminated. The good agreement between Jacobs' and Budyko's values over oceans provides some weak evidence that eddy effects are unimportant.

In the radiation computations there are several oppor-

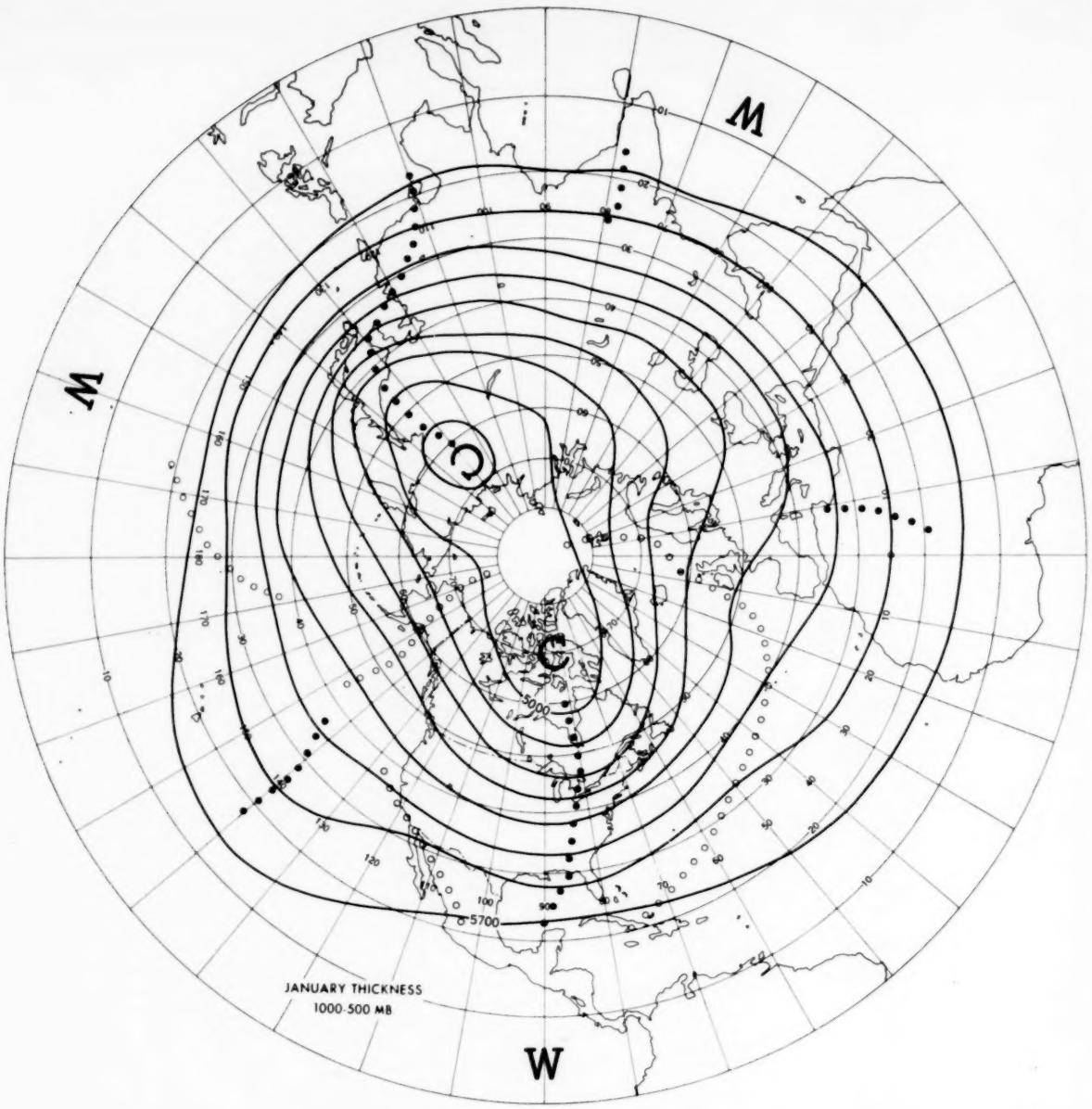

FIGURE 6.—Normal January thickness, 1,000 to 500 mb., after Jacobs [13]. Lines drawn for every 100 meters and labeled in meters. Centers of minimum thickness labeled C; maximum, W.

tunities for correlations to arise between parameters such as the albedo and short-wave radiation reaching the ground. Budyko [6] has attempted to make estimates of the errors arising in various steps of the radiation budget at the ground. He concludes that there is a 5 to 10 percent error in the monthly values of short-wave radiation, but that larger errors arise in the total budget because of irregular variations in albedo and surface temperature. However, in comparing estimates of total radiation with direct instrumental observations for a few Russian stations, he gets what he terms "very satisfactory" agreement. His computations also agree with the independent calculations by others.

Thus we may conclude that eddy effects play a relatively minor role in the heat-balance method.

5. THE ENERGY SOURCE FOR THE CIRCULATION

The two independent heating patterns (figs. 1 and 5) are quite dissimilar in their details, but their large-scale features are qualitatively alike, and show a similar overall

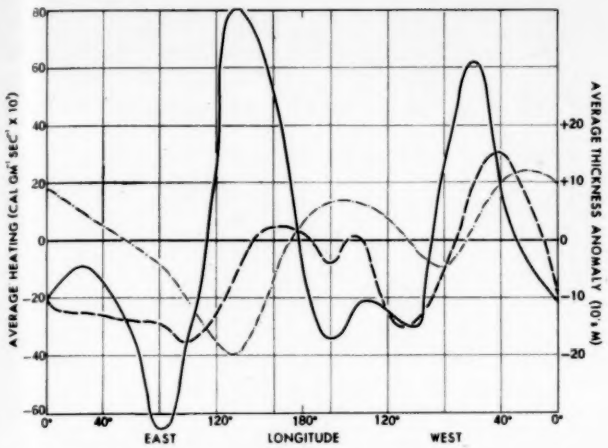

FIGURE 7.—Average normal winter heating and thickness in the layer 1,000 to 500 mb. and in the latitude band 30° N. to 60° N. as a function of longitude. Solid curve, heating by the thermodynamic energy equation method. Dashed curve, heating by the heat-balance method. Dash-dot curve, thickness departure from latitude average.

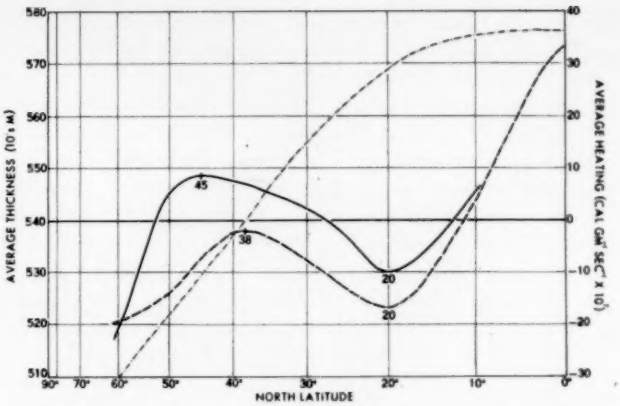

FIGURE 8.—Zonal averages of normal winter heating and thickness in the layer 1,000 to 500 mb. as a function of the sine of latitude. Solid curve, heating by the thermodynamic energy equation method. Dashed curve, heating by the heat-balance method. Dash-dot curve, thickness. Latitudes of maxima and minima of heating indicated.

relationship to the mean temperature field in the lower troposphere, portrayed here by the normal thickness between 1000 and 500 mb. (fig. 6). The latter has been constructed from normal data recently published by I. Jacobs [13].

Both heating patterns show a broad ring of maximum heating near the equator, associated with the highest tropospheric temperatures; maxima in middle latitudes in and to the east of the thermal troughs along the coasts of Asia and North America, and in the central Mediterranean; and cooling in and to the east of the long-wave ridges in western North America and the eastern Atlantic. Both charts show a broad region of cooling over the Eurasian continent associated with a rather flat west-to-east thermal pattern.

These large-scale relationships are brought out more clearly at middle latitudes in figure 7, which shows the average thickness and heating in the belt 30° N. to 60° N. plotted as a function of longitude. The curve of heating by the thermodynamic energy equation method agrees in almost all details with an independent computation by Wiin-Nielsen [32].

Figure 7 also emphasizes the considerable difference in magnitudes of heating and cooling by the two methods and shows an important phase difference between them. The maxima and minima of heating by the thermodynamic method are displaced 10° to 20° of longitude farther to the west. This seemingly small phase difference is quite important when considering the energy budget of the circulation. Lorenz [18] has shown that in order to get a positive transformation from thermal to potential energy, which is available for driving the circulation, there must be a positive correlation between heating and temperature. But the correlation between these two quantities, as portrayed in figure 7, is negative (−0.42) according to the thermodynamic and positive (+0.39) according to the heat-balance method. Thus, depending on which method is assumed correct, one may conclude that the semipermanent circulation in middle latitudes in winter is either energy-consuming or energy-producing. From the previous arguments in Sections 3 and 4 it is probable that the maximum heating centers of the thermodynamic method are too far west, while the pattern obtained from the heat-balance method is essentially correct. Thus, it is concluded that the semipermanent systems are energy-producing on the average. Some further interesting details of the energy budget will be given in later paragraphs.

Figure 8 shows the zonal averages of heating and thickness plotted against a sine function of latitude in order that a unit distance on the abscissa may represent a fixed area on the earth. Both of the heating curves show a positive correlation between thickness and heating south of 20° N. and north of 45° N. According to the equations of Lorenz [18], this means that in these regions there is a positive transformation between zonal heating and zonal available potential energy. The cooling at 20° N. and heating at the equator, shown in figure 8, may be identified with the sink and source of heat for the Hadley Cell, the thermally directed meridional circulation of low latitudes. The results of this study indicate that there is a positive transformation between heating and zonal potential energy at these latitudes, providing an important source of energy for the Hadley Cell. This is in agreement with a study by Tucker [30] which indicates that within the Hadley Cell there is also a positive transformation between zonal potential and zonal kinetic energy.

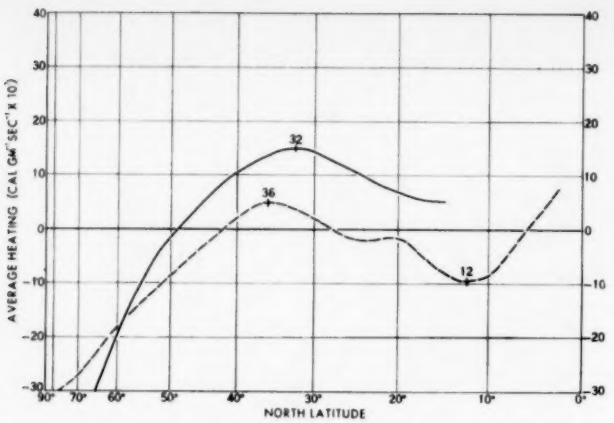

FIGURE 9.—Normal winter heating as a function of the sine of latitude after Pisharoty [27], solid curve; and after Gabites [10], dashed curve. See text for explanation.

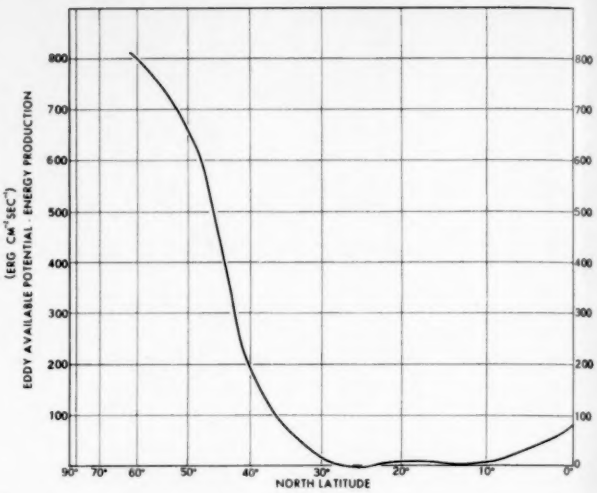

FIGURE 10.—Production of eddy available potential energy by the covariance of normal mean temperature and normal heating for winter, plotted as a function of the sine of latitude.

It is possible to provide a rough check on the validity of the latitudinal heating curves by comparing them with other studies. Two of these are summarized in figure 9, although unfortunately neither one has been computed for the same atmospheric layer, period of time, or heating components as those in figure 8. The reader must be referred to the sources for a discussion of the assumptions and approximations of these two estimates.

The first estimate, shown as the solid curve in figure 9, represents the horizontal geostrophic flux-divergence of heat in the layer 1000–200 mb. and for January and February 1949 (Pisharoty [26]). This omits the flux-divergence of heat by the meridional cells. The second estimate, shown as the dashed curve in figure 9, gives the normal heat-balance for January for the entire earth-atmosphere system (Gabites [10]). In addition to the average individual heating for the entire atmosphere, this includes heating in the oceans, measured by the latitudinal flux-divergence of heat produced by ocean currents.

Comparing these curves with those in figure 8, we note that there is good overall agreement in the location of the maxima and minima of heating. The curves of figure 9 are in better agreement with the magnitude of the heating maximum in middle latitudes obtained by the thermodynamic method, and suggest that the corresponding "maximum" for the heat-balance method is much too low. On the other hand, they are in better agreement with the location (phase) of the mid-latitude heating "maximum" for the heat-balance method. Both of these observations are in agreement with conclusions reached earlier from an analysis of the two procedures.

Finally, it is of some interest to attempt a more detailed quantitative analysis of the thermal energy budget of the semipermanent systems using the heating fields computed by the heat-balance method. The reader is referred to the original paper of Lorenz [18] for derivation of the energy transformation functions. Here, a somewhat different derivation by A. Wiin-Nielsen (unpublished lecture notes) has been used. This shows that the transformation between total heating and total available potential energy per unit area is given by the equation:

$$C=\frac{\Delta p}{S\overline{T}g}\int_S \overline{T}^*\frac{\overline{dq}^*}{dt}\,dxdy. \tag{4}$$

Here, C is a measure of the production of total available potential energy by the semipermanent systems (energy from this source which is available for maintaining the total mean circulation against friction); Δp, the pressure thickness of a thin vertical layer of the atmosphere; T and $\frac{dq}{dt}$, the absolute temperature and individual heating in the layer; and S, the area of the earth's surface for which the mean energy transformation is to be computed. The asterisk represents departure of a quantity from its area average, and the bar overscore, as before, represents an average in time.

Following Lorenz, one can divide the total energy production into two components: One is the production of eddy available potential energy (energy available for maintaining the semipermanent long waves); and the other the production of zonal available potential energy (energy available for maintaining the north-south temperature gradient). The production of eddy available energy is obtained simply by replacing $\overline{T}^*$ and $\frac{\overline{dq}^*}{dt}$ by the departure of each quantity from its zonal average; while each of these two quantities is replaced by the departure of its zonal average from its area average in order to compute the production of zonal available energy.

TABLE 1.—*Computation of total, eddy, and zonal available potential energy production per unit area in two selected latitude belts of the Northern Hemisphere for winter.* (*Units are ergs cm.$^{-2}$ sec.$^{-1}$*)

Latitude belt	Energy Production		
	Eddy	Zonal	Total
0° to 60° N.	+174	+275	+449
30° N. to 60° N.	+382	+223	+606

In this study it has been assumed that the mean temperature and heating do not vary in the vertical through the 1000- to 500-mb. layer, so that Δp is equal to 500 mb. Also, the mean temperature in the denominator of the coefficient has been set equal to a constant.

Figure 10 was computed from equation (4) using the data of figures 5 and 6, and shows the production of eddy available potential energy per unit area as a function of latitude. This suggests that at low latitudes the semipermanent long waves provide only a small fraction of the energy necessary for their own maintenance. Most of this energy must come from other sources, such as that generated by eddies of smaller time scale. However, north of 40° N., the energy produced by the semipermanent waves increases rapidly, until at 60° N. it is the same order of magnitude as that removed by friction. The latter is either 2000 or 4000 ergs cm.$^{-2}$ sec.$^{-1}$, depending on whether one accepts the estimates of Pisharoty [26] or of Brunt [4].

The total energy production (per unit area) and its two components have been computed for the entire area of the Northern Hemisphere between the equator and 60° N., and in the mid-latitude westerly belt between 30° N. and 60° N. The results are summarized in table 1.

Qualitatively, this table shows results which are to be expected from other considerations: in the region of the Hadley Cell and other meridional cells, a relatively large amount of zonal energy is produced. This is the bulk of the total energy production for the whole area and especially at low latitudes, while the relative importance of the zonal energy production diminishes greatly at higher latitudes. Perhaps somewhat surprising is the result that more total energy is produced per unit area at high than at low latitudes.

The relatively small magnitudes in table 1 are of some concern. The largest is only about 10 to 20 percent of the average frictional dissipation. This suggests that even at high latitudes the semipermanent circulations must be supported by energy from systems of smaller time scale, perhaps that produced in the traveling cyclones and anticyclones. However, these figures are probably much too small for two reasons: the magnitudes of the heating maxima at middle latitudes are too small, as concluded in this and previous sections; and there is a very important positive correlation between heating and temperature in the vertical, contrary to one of the assumptions made in evaluating equation (4). The vertical distribution of temperature and heating is important for the semipermanent long waves as well as for the meridional cells. This must be especially true for the Hadley Cell, where all the heat of condensation is released in the lower troposphere in the Doldrum belt, while the principal heat sink is at the top of a strong moisture discontinuity in the upper troposphere. If these two corrections could be included, they would result in a marked increase in the covariance between heating and temperature when integrated both horizontally and vertically over the selected region

6. CONCLUSIONS

There are differences in important details of the two normal heating patterns (figs. 1 and 5), which indicates that either or both of them are in error. However, they agree that the phase difference between the normal heating and temperature fields is close to 90°. Therefore, any procedure used in computing the heat budget must at least yield a good estimate of the *pattern* of heating, because a small error in pattern can change the sign of the energy transformation. Also, it must be clear that theoretical heating functions used in proposed general circulation models must also adhere to this critical phase relationship if they are to be at all realistic.

Future estimates of the thermal budget should be made by a fresh attack using the heat-balance approach, and they should include the vertical as well as the horizontal distribution of heating. Sources and sinks of energy for the summer season and for the Southern Hemisphere should also be considered.

ACKNOWLEDGMENTS

The assistance, criticism, and encouragement of several of the author's colleagues were essential in the completion of this report. Special thanks are due to Mr. Cecil Simmons, who provided technical assistance and advice; to Mrs. Georgia Campbell, who performed all the statistical computations; to Mrs. Jane Hess, Miss Rosemary Horning, and Mrs. Jacqueline Granville, who typed the manuscript; and to Mr. Roy Topper, who drafted the figures.

REFERENCES

1. F. Albrecht, "Untersuchungen über den Wärmehaushalt der Erdatmosphäre und seine Thermodynamische Bedeutung," *Berichte des Deutschen Wetterdeinstes in der U.S. Zone*, vol. 3, No. 17, 1950, 70 pp.
2. E. J. Aubert and J. S. Winston, "A Study of Atmospheric Heat Sources in the Northern Hemisphere for Monthly Periods," *Journal of Meteorology*, vol. 8, No. 2, Apr. 1951, pp. 111–125.
3. F. Bernhardt and H. Phillips, "Die Raumliche und Zeitliche Verteilung der Einstrahlung, der Ausstrahlung und der Strahlungsbilanz im Meeresniveau, Teil 1, Die Einstrahlung," *Abhandlungen des Meteorologischen und Hydrologischen Dienstes*, Deutsche Demokratische Republik, Nr. 45, Akademie-Verlag, Berlin, 1958, 227 pp.
4. D. Brunt, *Physical and Dynamical Meteorology*, Cambridge, England, 1939, 428 pp. (pp. 285–286).

5. M. I. Budyko, editor, *Atlas of the Heat Balance*, [Atlas Teplovogo Balansa] Glavnifi Geofizicheskafi Observatorifi im. A. I. Voeĭkova, Leningrad, 1955, 41 pp.,
6. M. I. Budyko, *The Heat Balance of the Earth's Surface*, [Teplovoĭ Balans Zemnoĭ Poverkhnosti] Hydrometeorological Publishing House, Leningrad, 1956, 254 pp. (Translated from the original Russian by N. A. Stepanova, U.S. Weather Bureau, 1958.)
7. J. Charney, "On the General Circulation of the Atmosphere," pp. 178–193 of *The Atmosphere and the Sea in Motion*, C.-G. Rossby Memorial Volume, The Rockefeller Institute Press in association with Oxford University Press, New York, 1959.
8. R. D. Elliott and T. B. Smith, "A Study of the Effects of Large Blocking Highs on the General Circulation in the Northern-Hemisphere Westerlies," *Journal of Meteorology*, vol. 6, No. 2, April 1949, pp. 67–85.
9. R. Fjørtoft, "Some Results Concerning the Distribution and Total Amount of Kinetic Energy in the Atmosphere as a Function of External Heat Sources and Ground Friction," pp. 194–211 of *The Atmosphere and the Sea in Motion*, C.-G. Rossby Memorial Volume, The Rockefeller Institute Press in association with Oxford University Press, New York, 1959.
10. J. F. Gabites, "Seasonal Variations in the Atmospheric Heat Balance," unpublished Doctor of Science thesis, Massachusetts Institute of Technology, 1950, 96 pp.
11. C. L. Godske, T. Bergeron, J. Bjerknes, and R. C. Bundgaard, *Dynamic Meteorology and Weather Forecasting*, American Meteorological Society, Boston, Mass., 1957, 800 pp. (p. 474).
12. K. J. Hanson, "Radiation Measurement on the Antarctic Snowfield, A Preliminary Report," *Journal of Geophysical Research*, vol. 65, No. 3, Mar. 1960, pp. 935–946.
13. I. Jacobs, "5-Resp. 40-Year Monthly Means of the Absolute Topographies of the 1000-mb., 850-mb., 500-mb., and 300-mb. Levels and of the Relative Topographies 500/1000 mb. and 300/500 mb. over the Northern Hemisphere and their Month-to-Month Changes," Institut für Meteorologie und Geophysik der Freien Universität, Berlin, vol. 1, 1957.
14. W. C. Jacobs, "The Energy Exchange between Sea and Atmosphere and Some of its Consequences," *Bulletin of the Scripps Institution of Oceanography*, vol. 6, No. 2, 1951, pp. 27–122.
15. C. E. Jensen, "Energy Transformations and Vertical Flux Processes over the Northern Hemisphere," *Scientific Report* No. 1, Planetary Circulations Project, Massachusetts Institute of Technology, August 1960, 271 pp.
16. H. Landsberg, "Climatology," Chapter XII in *Handbook of Meteorology*, F. A. Berry, E. Bollay, and N. R. Beers, editors, McGraw-Hill Book Co., Inc., New York, 1945, pp. 927–997.
17. J. London, "A Study of the Atmospheric Heat Balance," *Final Report*, Contract AF19(122)-165, Dept. of Meterology and Oceanography, New York University, July 1957, 99 pp.
18. E. N. Lorenz, "Available Potential Energy and the Maintenance of the General Circulation," *Tellus*, vol. 7, No. 2, May 1955, pp. 157–167.
19. D. E. Martin, "An Investigation of Systematic Errors in the Barotropic Forecasts," *Tellus*, vol. 10, No. 4, Nov. 1958, pp. 451–465.
20. Y. Mintz, "Design of Some Numerical General Circulation Experiments," *Bulletin of the Research Council of Israel*, vol. 7G, No. 2–3, Oct. 1958, pp. 67–114.
21. F. Möller, "Die Wärmebilanz der Freien Atmosphäre im Januar," *Meteorologische Rundschau*, vol. 3, No. 5/6, 1950, pp. 97–108.
22. F. Möller, "Vierteljahrskarten des Niederschlags für die Ganze Erde," *Petermanns Geographische Mitteilungen*, vol. 95, No. 1, 1951, pp. 1–7.
23. F. Möller, "Radiation and Meteorology," presented at meeting of the Radiation Commission of International Association of Meteorology and Atmospheric Physics, Oxford, July 20, 1959, 10 pp.
24. H. A. Panofsky, "Large-Scale Vertical Velocity and Divergence," *Compendium of Meteorology*, American Meteorological Society, Boston, 1951, pp. 639–646.
25. N. A. Phillips, "The General Circulation of the Atmosphere: A Numerical Experiment," *Quarterly Journal of the Royal Meteorological Society*, vol. 82, No. 352, April 1956, pp. 123–164.
26. P. R. Pisharoty, "The Kinetic Energy of the Atmosphere," Article XIV in *Final Report*, Contract AF 19(122)–48, Dept. of Meteorology, University of California at Los Angeles, March 1955.
27. P. R. Pisharoty, "Some Aspects of the Geostrophic Poleward Flux of Sensible Heat," Article XV in *Final Report*, Contract AF 19(122)–48, Dept. of Meteorology, University of California at Los Angeles, March 1955.
28. G. C. Simpson, "The Distribution of Terrestrial Radiation," *Memoirs of the Royal Meteorological Society*, vol. 3, No. 23, Apr. 1929, pp. 53–78.
29. Staff Members Academia Sinica, Institute of Geophysics and Meteorology, Peking, "On the General Circulation of Eastern Asia (III)," *Tellus*, vol. 10, No. 3, Aug. 1958, pp. 299–312.
30. G. B. Tucker, "Mean Meridional Circulations in the Atmosphere," *Quarterly Journal of the Royal Meteorological Society*, vol. 85, No. 365, July 1959, pp. 209–224.
31. H. Wexler, "Determination of the Normal Regions of Heating and Cooling in the Atmosphere by Means of Aerological Data," *Journal of Meteorology*, vol. 1, Nos. 1 and 2, Sept. 1944, pp. 23–28.
32. A. Wiin-Nielsen, "A Study of Energy Conversion and Meridional Circulation for the Large-Scale Motion in the Atmosphere," *Monthly Weather Review*, vol. 87, No. 9, Sept. 1959, pp. 319–332.

LEE-SIDE FRONTOGENESIS IN THE ROCKY MOUNTAINS[1]

TOBY N. CARLSON

Department of Meteorology, Massachusetts Institute of Technology, Cambridge, Mass.

[Manuscript received January 17, 1961; revised March 6, 1961]

ABSTRACT

The development and motion of fronts associated with lee-side troughs on large mountain barriers has been investigated. These fronts differ from ordinary cold fronts in their horizontal temperature field, which is characterized by a sinusoidal thermal ridge. The thermal ridge intensifies, while remaining stationary with respect to the mountains, and moves eastward upon the approach of a Pacific cold front.

An equation is derived, showing that changes in the thermal pattern can be described by changes in a potential thermal vorticity equation, which consists of three terms: (1) one representing an advection of the potential thermal vorticity by the 500-mb. wind; (2) one representing the advection of 500-mb. absolute vorticity by the thermal wind; and (3) a purely orographic term.

An idealized sinusoidal model of the thickness pattern is used in conjunction with the prognostic equation to explain the development and motion of lee-side thermal ridges. Actual examples from synoptic maps are chosen to corroborate the theory. The conclusions are: (1) the thermal ridge will develop when the surface flow is such as to produce large-scale descent on the lee slopes of the mountains; (2) no thermal ridging will appear when the 500-mb. ridge lies east of the lee slopes; (3) thermal ridging will appear with the approach of a 500-mb. ridge from the west; and (4) the thermal ridge will move eastward upon the passage of the 500-mb. ridge.

1. INTRODUCTION

A well-known phenomenon is the lee-side trough, associated with large mountain barriers. At certain times of the year low-pressure troughs frequently develop on the eastern slopes of the Rocky Mountains. A particular type of front can be found along the axis of the trough, which is distinguishable from ordinary cold or warm fronts by its horizontal temperature field. This kind of front will be called a "pseudo front" in this paper. Here the word "pseudo" is not to be confused with other definitions involving the term, as applied to squall lines and other meso-features [1]. Typically, cold fronts lie along the axes of low-pressure troughs, moving from colder to warmer air. In a typical cold front the thermal gradient is quite pronounced behind the front (fig. 1). Pseudo fronts differ from cold fronts in that (1) the associated surface trough does not show an abrupt temperature discontinuity at low levels, although the wind shift across the front may be quite pronounced, and (2) the thermal contours are almost symmetrical about the surface trough axis, with a maximum temperature at the front, decreasing at about the same rate on either side of the trough. It is evident that this description is exactly that of the temperature field associated with an occluded front. Pseudo fronts are distinguished from occlusions on the

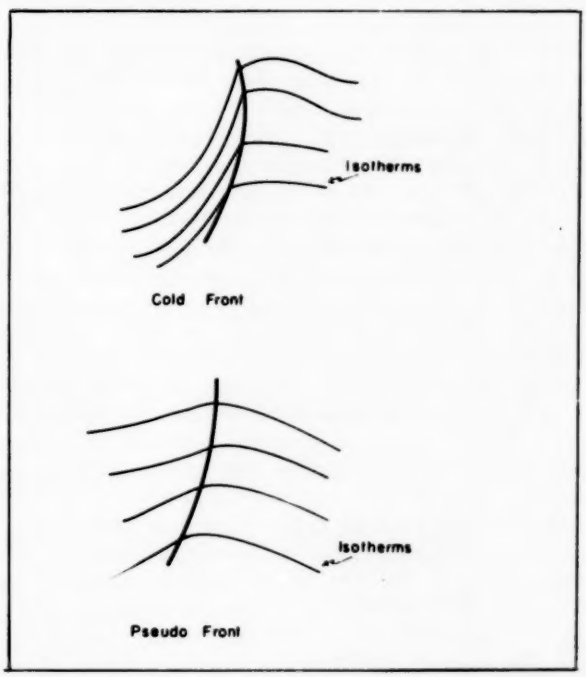

FIGURE 1.—Schematic diagrams of cold and pseudo fronts.

[1] Based on a Master's Thesis in the Department of Meteorology, Massachusetts Institute of Technology, and part of a project prepared for the Air Force Cambridge Research Laboratories, Contract AF(604)-5491.

588203—61——3

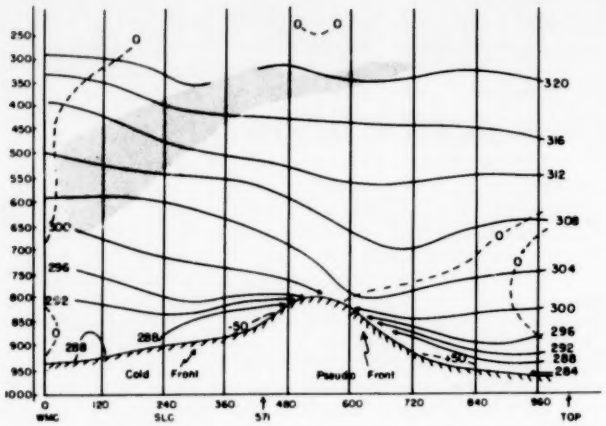

FIGURE 2.—Cross-section, Winnemucca, Nev. (WMC), to Topeka, Kans. (TOP), 1200 GMT, January 13, 1959. Solid lines are isotherms of potential temperature; dashed lines, vertical velocity, mb. (12 hr.)$^{-1}$. Shading indicates greater than three-eighths cloud cover. Distance is in miles.

basis of the development of the latter in the life of a frontal wave. In the early stages of cyclogenesis, the thermal structure of a pseudo front often resembles that of an occlusion, except that the system is intensifying. There seems to be no evidence in the historical continuity of pseudo fronts that a cold front has overtaken a warm front, such as occurs toward the end of the evolutionary cycle of a classical Bergeron cyclone.

The most common type of pseudo front on the North American continent develops along the lee slopes of the Rocky Mountains, particularly during the months of November through March. The front first appears in the thermal pattern as a sinusoidal ridge, with a wavelength of about 1500 km. At the surface, a marked wind shift line appears coincident with the thermal ridge axis. The wave intensifies in both the thermal and surface circulations, often becoming extended along the entire eastern slopes of the mountains, although during initial development the forward advance is often very slight. McClain [2] and Hess and Wagner [3] have studied in detail the development of lee-side cyclogenesis, and their analyses of 12-hour synoptic maps showed that the lee cyclones began to move eastward upon the approach of a trough from the Pacific. Cloudiness and precipitation accompanying the front are noticeably absent [4]. A cross-section through both the approaching cold front from the Pacific and the pseudo front at 1200 GMT, January 13, 1959, reveals not only the total lack of middle cloudiness and precipitation accompanying the pseudo front, but points out its distinct identity in the temperature field (fig. 2). The phenomenon of the lee-side pressure trough is of such frequent occurrence in the Rocky Mountain region, that mean sea level charts show it clearly [3]. The time required for full development of a lee-side trough is about 36 hours, and the rapid intensification of the thermal ridge east of the Rocky Mountains is associated with the commonly experienced "chinook" or "foehn." The ultimate eastward movement of the pseudo front seems to be influenced by approaching Pacific troughs.

The purpose of this paper is to try to explain the development and movement of these pseudo fronts in terms of the large-scale physical processes in the atmosphere. Similar work has been done by McClain [2], in which he correlated upper tropospheric divergence with the development of the lee-side troughs. Other researchers such as Colson [5] and Newton [6] have tried to explain the frequency of cyclogenesis in the central United States in terms of air flow over the Rocky Mountains.

2. THEORY

Since pseudo fronts are best revealed in the low-level temperature pattern, it becomes necessary to discuss the motion of the accompanying thermal ridge. It would be best to derive a comprehensive prediction equation for the thickness pattern, from the basic laws governing the atmosphere. One approach, which works reasonably well and is simple, is use of a two-parameter model which describes the atmosphere in terms of the mean wind and a thermal wind, taken over an appropriate depth in the atmosphere. The following modeling assumption is chosen:

$$\mathbf{V}(x, y, p, t)=\mathbf{V}_m(x, y, t)+B(p)\mathbf{V}_{m0}(x, y, t) \tag{1}$$

where $\mathbf{V}$ refers to the non-divergent component of the wind, and B is a function of pressure only. The definition of the mean quantities is written

$$(\ )_m\equiv\frac{1}{p_0}\int_0^{p_0}(\ )dp. \tag{2a}$$

The subscripts m and 0 respectively refer to the mean and 1000-mb. levels, where

$$(\ )_{m0}\equiv(\ )_m-(\ )_0. \tag{2b}$$

From the previous definitions, it is evident that $B_m=0$ and that the vertical shear is constant in a particular air column. Applying the curl operator to (1) gives the corollary

$$\zeta=\zeta_m+B\zeta_{m0}, \tag{3}$$

where ζ is the relative vorticity component in the vertical. Introduction of the simplified vorticity equation

$$\frac{\partial\zeta}{\partial t}=-\mathbf{V}\cdot\nabla(\zeta+f)+f\frac{\partial\omega}{\partial p}, \tag{4}$$

where ∇ is the gradient operator at constant pressure, $\omega\equiv\frac{dp}{dt}$, and f is the Coriolis parameter, yields an expres-

sion for large-scale atmospheric motion. The simplification refers to the deletion of the twisting, vertical advection, and frictional terms, and the assumption that $f \gg \zeta$. The boundary conditions for the model atmosphere are:

$$\omega(p=0)=0, \tag{5a}$$

$$\omega(p=p_s)=\omega_s \tag{5b}$$

where subscript s refers to the ground surface. Substitution of (1) and (3) in (4) yields

$$\frac{\partial \zeta_m}{\partial t}+B\frac{\partial \zeta_{m0}}{\partial t}=-\mathbf{V}_m\cdot\nabla(\zeta_m+f)-B\mathbf{V}_m\cdot\nabla\zeta_{m0} -B\mathbf{V}_{m0}\cdot\nabla(\zeta_m+f)-B^2\mathbf{V}_{m0}\cdot\nabla\zeta_{m0}+f\frac{\partial\omega}{\partial p}. \tag{6}$$

To eliminate $\frac{\partial \zeta_m}{\partial t}$, apply (2) to (4), obtaining another expression for $\frac{\partial \zeta_m}{\partial t}$ and subtract the result from (6). Thus,

$$\frac{\partial \zeta_{m0}}{\partial t}=-\mathbf{V}_{m0}\cdot\nabla(\zeta_m+f)-\left\{\mathbf{V}_m+\mathbf{V}_{m0}\left[\frac{B^2-(B^2)_m}{B}\right]\right\}\cdot\nabla\zeta_{m0} +\frac{f}{B}\left(\frac{\partial\omega}{\partial p}\right)-\frac{f}{B}\frac{\omega_s}{p_s}. \tag{7}$$

Application of this equation at the level where $B^2=(B^2)_m$ and defining $B_*\equiv\sqrt{(B^2)_m}$ yields:

$$\frac{\partial \zeta_{m0}}{\partial t}=-\mathbf{V}_{m0}\cdot\nabla(\zeta_m+f)-\mathbf{V}_m\cdot\nabla\zeta_{m0}+\frac{f}{B_*}\left(\frac{\partial\omega}{\partial p}\right)_*-\frac{f}{B_*}\frac{\omega_s}{p_s}. \tag{8}$$

Terms containing ω can be eliminated by introduction of the thermodynamic considerations. For a temperature field where the potential temperature $\theta=\theta(x,y,p,t)$,

$$\frac{d\theta}{dt}=\frac{\partial\theta}{\partial t}+\mathbf{V}\cdot\nabla\theta+\omega\frac{\partial\theta}{\partial p}. \tag{9}$$

The quantity θ is defined in the usual manner where

$$\theta\equiv T\left(\frac{p_0}{p}\right)^{\kappa}=\frac{\alpha}{R}\frac{p_0^{\kappa}}{p^{\kappa-1}}, \tag{10}$$

where T is the absolute temperature, α the specific volume, R the gas constant for dry air, $p_0=1000$ mb., and $\kappa\equiv R/c_p$. Since $\left(\frac{\partial\theta}{\partial t}\right)_p=\frac{\theta}{\alpha}\left(\frac{\partial\alpha}{\partial t}\right)$ and $\nabla\theta=\theta/\alpha\nabla\alpha$, equation (9) becomes, after multiplication by α/θ and substitution of these relationships

$$\frac{\alpha}{\theta}\frac{d\theta}{dt}=\frac{\partial\alpha}{\partial t}+\mathbf{V}\cdot\nabla\alpha+\frac{\alpha}{\theta}\frac{\partial\theta}{\partial p}\omega. \tag{11}$$

The requirement that the atmosphere be in hydrostatic equilibrium gives

$$\alpha=-g\frac{\partial z}{\partial p}, \tag{12}$$

where g is the gravitational constant and z is the height of a constant pressure surface. Substitution of (12) into (11) yields, upon division by g and rearrangement of terms

$$\frac{\partial}{\partial t}\left(\frac{\partial z}{\partial p}\right)=-\mathbf{V}\cdot\nabla\left(\frac{\partial z}{\partial p}\right)+\frac{\alpha}{g\theta}\frac{\partial\theta}{\partial p}\omega-\frac{\alpha}{g\theta}\frac{d\theta}{dt}. \tag{13}$$

Assuming that no non-adiabatic heating occurs, integration of (13) with respect to pressure from 1000 mb. to the mean level, where the pressure is p_m, yields

$$\frac{\partial z_{m0}}{\partial t}=-\mathbf{V}_m\cdot\nabla z_{m0}+\int_{1000}^{p_m}\frac{\alpha}{g\theta}\frac{\partial\theta}{\partial p}\omega dp, \tag{14}$$

since $\mathbf{V}_{m0}\cdot\nabla\left(\frac{\partial z}{\partial p}\right)=0$ and $\mathbf{V}\cdot\nabla\left(\frac{\partial z}{\partial p}\right)=\mathbf{V}_m\cdot\nabla\left(\frac{\partial z}{\partial p}\right)$. From the equation of continuity

$$\omega=-\int_0^p\nabla\cdot(\mathbf{V}_m+B\mathbf{V}_{m0})\,dp=\frac{p}{p_s}\omega_s-\nabla\cdot\mathbf{V}_{m0}\int_0^p Bdp. \tag{16}$$

Similarly

$$\left(\frac{\partial\omega}{\partial p}\right)_*=\frac{\omega_s}{p_s}-B_*\nabla\cdot\mathbf{V}_{m0}. \tag{17}$$

By substitution of (16) in (14), and defining $c\equiv\int_0^p Bdp$ the thermodynamic equation becomes

$$\frac{\partial z_{m0}}{\partial t}=-\mathbf{V}_m\cdot\nabla z_{m0}+\frac{\omega_s}{p_s}E-\nabla\cdot\mathbf{V}_{m0}D, \tag{18}$$

where $E\equiv\int_{1000}^{p_m}\frac{\alpha p}{g\theta}\frac{\partial\theta}{\partial p}\,dp$, and $D\equiv\int_{1000}^{p_m}\frac{c\alpha}{g\theta}\frac{\partial\theta}{\partial p}\,dp$. Substitution of (17) into (8) yields

$$\frac{\partial \zeta_{m0}}{\partial t}=-\mathbf{V}_{m0}\cdot\nabla(\zeta_m+f)-\mathbf{V}_m\cdot\nabla\zeta_{m0}-f\nabla\cdot\mathbf{V}_{m0}. \tag{19}$$

Elimination of $\nabla\cdot\mathbf{V}_{m0}$ between (18) and (19), and rearrangement of terms yields

$$\frac{\partial}{\partial t}\left(\zeta_{m0}-\frac{f}{D}z_{m0}\right)=-\mathbf{V}_m\cdot\nabla\left(\zeta_{m0}-\frac{f}{D}z_{m0}\right) -\mathbf{V}_{m0}\cdot\nabla(\zeta_m+f)-\frac{fE\omega_s}{p_sD}, \tag{20}$$

which can be written in the abbreviated form

$$\frac{\partial}{\partial t}(\zeta_{m0}-Kz_{m0})=-\mathbf{V}_m\cdot\nabla(\zeta_{m0}-Kz_{m0})-\mathbf{V}_{m0}\cdot\nabla(\zeta_m+f)-k\omega_s, \tag{21}$$

where $K\equiv f/D$ and $k\equiv fE/(p_sD)$. E and D can be evaluated from Buch's [7] mean data, and from mean values of $\partial\theta/\partial p$ for western North America.

In a typical synoptic situation, changes in ζ_{m0} and $-Kz_{m0}$ augment each other since increases or decreases in thermal vorticity are associated, respectively, with decreases or increases in thickness. The combined expression $(\zeta_{m0}-Kz_{m0})$ can be called a potential thermal vorticity. This means that the thermal vorticity ζ_{m0} has a potential value with respect to some value of z_{m0}. Using the symbol ϕ for the potential thermal vorticity, expression (21) becomes

$$\frac{\partial \phi}{\partial t}=-\mathbf{V}_m\cdot\nabla\phi-\mathbf{V}_{m0}\cdot\nabla(\zeta_m+f)-k\omega_s, \tag{22}$$

or

$$\frac{d\phi}{dt}=-\mathbf{V}_{m0}\cdot\nabla(\zeta_m+f)-k\omega_s. \tag{23}$$

The terms $-\mathbf{V}_{m0}\cdot\nabla(\zeta_m+f)$ and $-k\omega_s$ represent nonconservative, or generative, effects. The presence of generative terms suggests a means by which thermal ridges are suddenly built up on the lee slopes of large mountain ranges. The former term is not localized geographically, so that $-k\omega_s$ must represent the effect which is responsible for the lee-slope development. It is conceivable that the orographic contribution can influence the thermal pattern in such a way that $-\mathbf{V}_{m0}\cdot\nabla(\zeta_m+f)$ itself is altered, making that a secondary effect of the orography. Since ω_s is positive for winds blowing from higher to lower levels, downslope winds will always contribute negatively to $\partial\phi/\partial t$ and increase thermal ridging.

The entire expression (22) is quite consistent with other types of manipulation of the two-parameter model atmosphere, such as those employed by Sawyer and Bushby [8] and Sutcliffe [9], but is more appropriate for the present problem in that it refers explicitly to the thermal pattern. Equation (21) is not limited to orographic effects, and can be utilized to study any kind of large-scale thermal pattern. Consider a typical mid-latitude trough-ridge pattern at the mean level, where a low-level baroclinic cyclone appears on the eastern side of the upper trough. The isotherms associated with the surface Low will advance northward, becoming greatly extended, and finally become concentrically closed. Because of the close association between changes in the potential thermal vorticity and changes in the thickness, the first term on the right side of (21) explains the northward movement of the thermal pattern. Now, the origin of closed isotherms cannot be explained by a single horizontal advection process, and therefore, a second effect, such as that described by the last term on the right side of (23), must be responsible for the development of pools of cold and warm air. For this reason equation (21) could be appropriate in studying cold Lows and warm Highs.

3. THE IDEALIZED MODEL

Consider an ideal sinusoidal z_{m0} field as schematically represented in figure 3. The x-axis lies in the east-west direction, and the y-axis coincides with the north-south mountain ridge. The crest of the idealized thermal ridge coincides with x''. The following statement can then be made

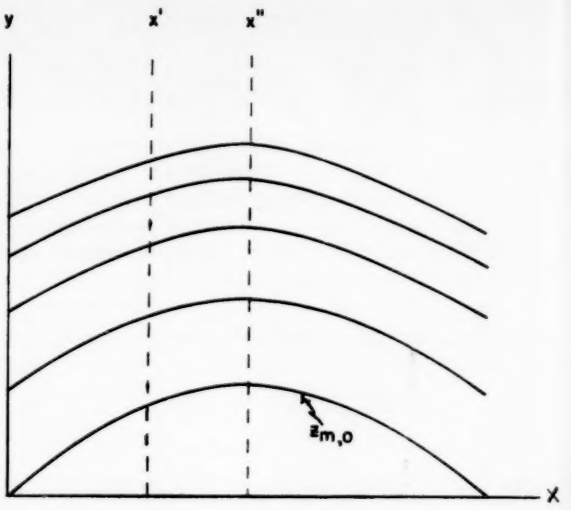

FIGURE 3.—Schematic model of ideal thickness pattern. Isolines of z_{m0} in the x, y plane. x''=axis of ridge. x'= position of maximum descent.

$$z_{m0}=a\sin\frac{2\pi x}{\lambda}+by, \tag{24}$$

where a is the amplitude of the ridge, λ the wavelength of the pattern, and b is taken to be a constant, although it generally slightly increases toward the north. Now if the geostrophic assumption holds,

$$\zeta_{m0}=\frac{g}{f}\nabla^2 z=-\frac{g}{f}\left(\frac{2\pi}{\lambda}\right)^2 a\sin\frac{2\pi x}{\lambda}. \tag{25}$$

The above expression indicates the resemblance between ϕ and z_{m0} since

$$\phi=a'\sin\frac{2\pi x}{\lambda}+b'y, \tag{26a}$$

where

$$a'\equiv-\left[\frac{g}{f}\left(\frac{2\pi}{\lambda}\right)^2+K\right]a, \text{ and } b'\equiv-K\,b. \tag{26b}$$

Consider a pattern of flow at the mean level, where the component of the mean wind $u_m\equiv U$, and v_m is represented by a perturbation v', and the term, $-\mathbf{V}_{m0}\cdot\nabla(\zeta_m+f)$ is represented by the symbol Q. The 500-mb. pattern consists of a steady zonal current with a speed U upon which is superimposed a transversal wave perturbation. The expression (21) becomes

$$\frac{\partial \phi}{\partial t}=-U\frac{\partial \phi}{\partial x}-v'\frac{\partial \phi}{\partial y}-k\omega_s+Q. \tag{27}$$

In order to determine the eastward movement of the thermal ridge, this equation is differentiated with respect to x at the point x'':

$$\frac{\partial}{\partial x}\left(\frac{\partial \phi}{\partial t}\right)_{x''}=-U\left[\left(\frac{2\pi}{\lambda}\right)^2\left\{\frac{g}{f}\left(\frac{2\pi}{\lambda}\right)^2+K\right\}\right]a -k\frac{\partial \omega_s}{\partial x}+\frac{\partial v'}{\partial x}Kb+\frac{\partial Q}{\partial x}. \tag{28}$$

The last two terms on the right side of (28) represent the influence on the motion of the thermal ridge by the perturbed part of the mean flow, and therefore demonstrate the effects of migratory troughs and ridges at the mean level. It is evident that $\partial v'/\partial x$ is merely ζ_m, and that the entire term, $Kb\zeta_m$, represents an advective influence by the non-zonal component of the mean wind. The last term represents a generating effect on thermal ridges by vorticity advection gradients at the mean level. Henceforth, these two terms will be combined as one, where $Q'\equiv Kb\zeta_m+\frac{\partial Q}{\partial x}$. From (28) the following conditions exist:

$$\frac{\partial}{\partial x}\left(\frac{\partial \phi}{\partial t}\right)_{x''}=0, \text{ stationarity} \tag{29a}$$

$$\frac{\partial}{\partial x}\left(\frac{\partial \phi}{\partial t}\right)_{x''}>0, \text{ quasi stationarity} \tag{29b}$$

$$\frac{\partial}{\partial x}\left(\frac{\partial \phi}{\partial t}\right)_{x''}<0, \text{ eastward movement} \tag{29c}$$

First consider the equation of stationarity: solving for a at x'', (28) becomes

$$a=\frac{-k\left(\frac{\partial \omega_s}{\partial x}\right)+Q'}{U\left[\left(\frac{2\pi}{\lambda}\right)^2\left\{\frac{g}{f}\left(\frac{2\pi}{\lambda}\right)^2+K\right\}\right]}=a_c. \tag{30}$$

If the magnitude of Q' is less than the magnitude of $k\frac{\partial \omega_s}{\partial x}$, $\frac{\partial \omega_s}{\partial x}$ must be a negative quantity in order for a to be positive. Thus stationary thermal ridges must become positioned where $\frac{\partial \omega_s}{\partial x}$ is negative, in particular at a point downstream from the region of maximum descent. Equation (30) states that there exists a positive finite amplitude which will satisfy the stationarity condition. This amplitude will be called the "critical amplitude" represented by the symbol a_c. Substitution of (30) in (28) yields

$$\frac{\partial}{\partial x}\left(\frac{\partial \phi}{\partial t}\right)_{x''}=U\left[\left(\frac{2\pi}{\lambda}\right)^2\left\{\frac{g}{f}\left(\frac{2\pi}{\lambda}\right)^2+K\right\}\right](a_c-a). \tag{31}$$

Equation (31) explicitly states that the thermal ridge will advance eastward, if $a_c>a$.

Consider the idealized development of a thermal ridge when a steady pattern of ω_s is imposed upon the lee slope of the mountain at $t=0$. The initial position of the ridge will be at x', since the generating effect of $-k\omega_s$ is greatest at that point. Now $\partial\omega_s/\partial x$ is zero at x', and therefore, according to (30) and (31), the ridge must move eastward in the first instant, but as it does so, a_c also increases according to (30). The term, $-k\omega_s$, represents an effect which is continuously generating a thermal ridge, and thus increasing the amplitude of the ridge with time. The critical amplitude can never exceed the actual amplitude without imposing the stationarity condition. Similarly, the actual amplitude can never greatly exceed the critical amplitude, since that quantity will also increase as the thermal ridge moves east of x'. If $a\approx a_c$, equation (31) states that an approximate condition of stationarity exists. Although the extent and duration of approximate stationarity cannot be shown, the condition will persist until the thermal ridge attains a position downstream from x', where $\partial\omega_s/\partial x$ is at a minimum. Further eastward movement will be accompanied by a rapid decrease in critical amplitude according to (30), and a negation of the condition of approximate stationarity.

The horizontal advection of ϕ represents a decrease in this quantity ahead of x'', and an increase behind it, while $-k\omega_s$ is decreasing ϕ ahead of x'', but is decreasing it more strongly at x'. The growing importance of the advection of ϕ causes the ridge to move slowly eastward. The ultimate reduction of the critical amplitude corresponds physically to the domination of the horizontal advection over the orographic process.

If Q' is negative across the ridge axis, the numerator in (30) will tend toward zero, leaving $a_c\ll a$. According to (31), this event will tend to remove an approximate stationarity condition which may be present. If no ridge is present, none may be allowed to form under such circumstances, since any amplitude which is created will be immediately advected downstream. Similarly, when Q' is positive, equation (30) states that the maximum critical amplitude will be much larger than in the situation where Q' is negative. In effect, this means that the approximate stationarity condition exists for a considerably longer time.

Since b is a negative constant in the present reference system, from the definition of Q', negative relative vorticity at the mean level contributes to stationarity. The generative effect of Q will also contribute to stationarity when $\partial Q/\partial x$ is positive, or when stronger cyclonic vorticity advection occurs east of the thermal ridge. Calculations of this term have shown its magnitude to be very small, and therefore Q' primarily consists of ζ_m. Thus Q' will tend to be strongly positive in the vicinity of a 500-mb. ridge, and begin to decrease sharply behind it.

In conclusion, it must be pointed out that (1) the initial

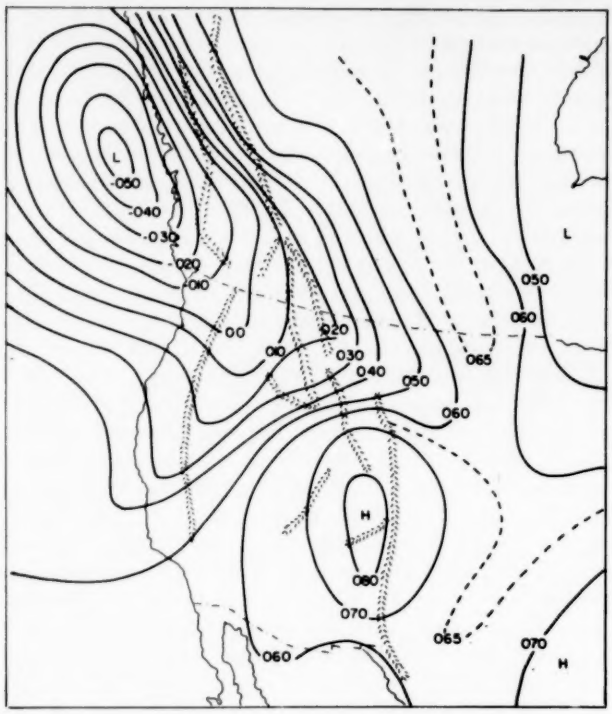

FIGURE 4.—1000-mb. height contours (ft.), 1200 GMT, January 12, 1959 (unit digits omitted).

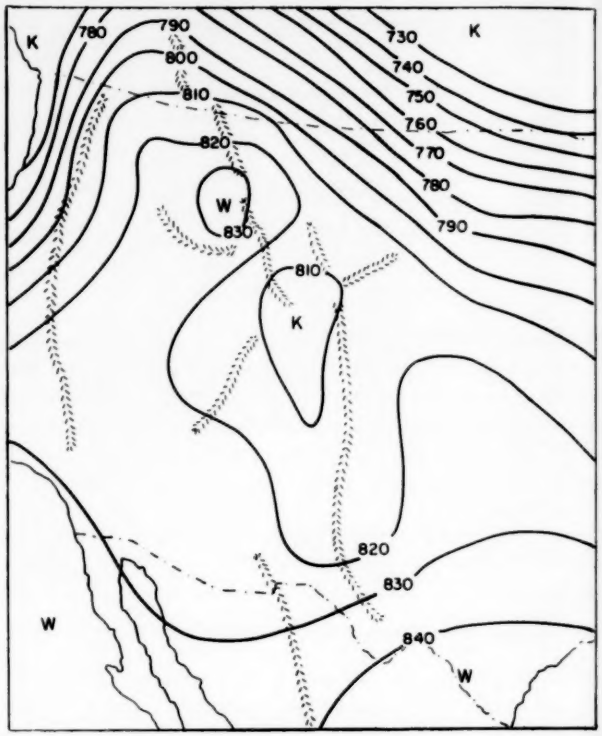

FIGURE 5.—1000–500-mb. thickness contours (ft.), 1200 GMT, January 12, 1959 (ten of thousands and unit digits omitted).

formation of a thermal ridge is dependent on the fundamental assumption that appreciable downslope velocities exist, and (2) the initial formation of the thermal ridge will not be observed as a lee-slope phenomenon if large positive values of relative vorticity at 500 mb. are occurring over the lee slopes of the mountain. If Q' is the largest in the numerator of (30) the position of the thermal ridge will not necessarily be localized on the east slope of the mountain range. Finally (3), the magnitude of both terms in the numerator of (30) will tend to vary with the wind speed, and therefore the critical amplitude may be somewhat insensitive to wind speed.

4. EXAMPLES OF LEE CYCLOGENESIS

A SPECIFIC CASE

An example of pseudo front development on the lee slopes of the Rocky Mountains has been chosen. The situation selected occurred between 1200 GMT, January 12, 1959, and 1200 GMT, January 13, 1959. The series of surface maps (figs. 4, 7, 10) reveals the development of the surface front. It was first noticed in connection with a feeble trough in the 065 contour in figure 4, and later exhibited a pronounced wind shift line, although no marked horizontal temperature contrast was present. The series of thickness maps (figs. 5, 8, 11) indicates the

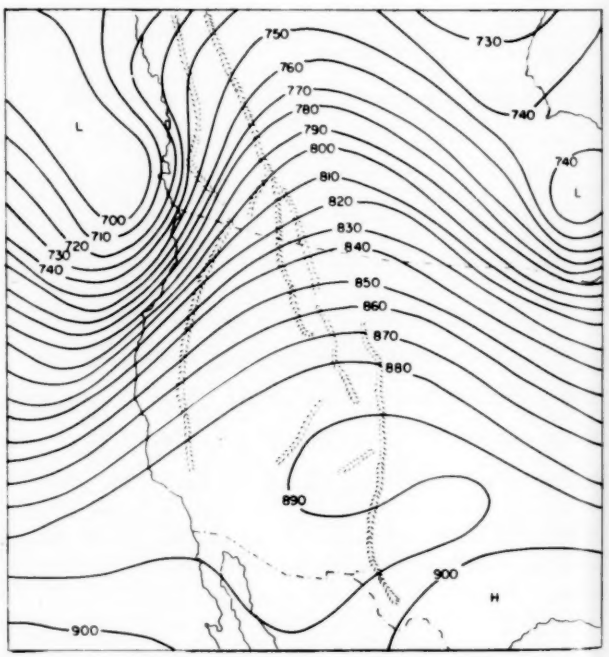

FIGURE 6.—500-mb. height contours (ft.), revealing strong cyclonic vorticity advection from the Pacific, 1200 GMT, January 12, 1959 (ten of thousands and unit digits omitted).

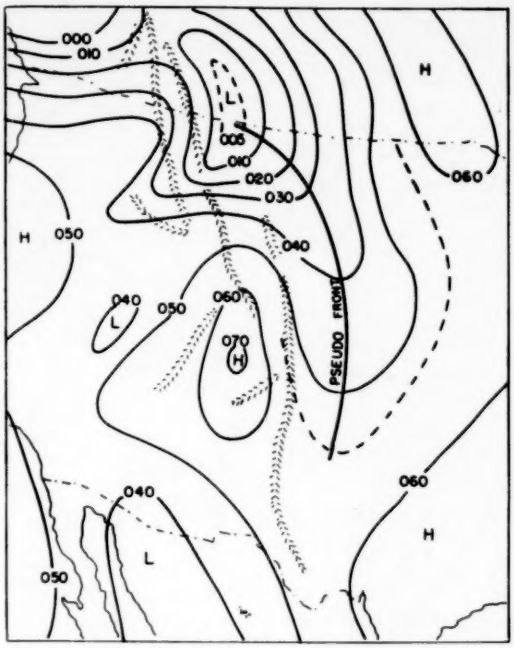

FIGURE 7.—1000-mb. height contours (ft.), 0000 GMT, January 13, 1959 (unit digits omitted).

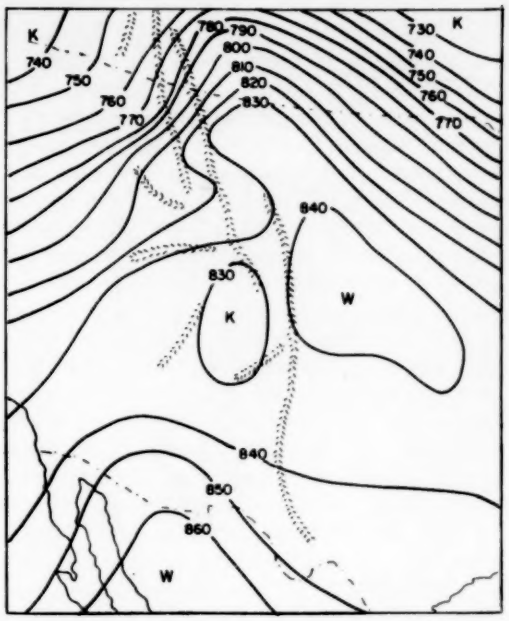

FIGURE 8.—1000–500-mb. thickness contours (ft.), 0000 GMT, January 13, 1959 (ten of thousands and unit digits omitted).

typical sinusoidal shape of the thermal pattern. Of note is the deep pocket of warm air around Colorado, associated with strong descending motion in that area. Although not presented here, maps preceding 1200 GMT, January 12, indicate the presence of a weak thermal ridge. Over Canada, the temperature field associated with the vigorous Pacific Low has apparently merged with the northern portion of the thermal ridge, and continued to move rapidly eastward. In terms of equation (30), the large cyclonic vorticity advection at 500 mb. (fig. 6) over southern Canada was removing the stationarity condition over the eastern slope of the mountain. South of the Canadian border, the 500-mb. ridge was positioned slightly west of the thermal ridge (figs. 9, 12). As the 500-mb. ridge moved east of the thermal ridge, the latter began to move eastward. This event could be anticipated by the idealized model, since Q' would tend to decrease sharply upon the passage of a 500-mb. ridge. Large Pacific Ocean cyclones which approach Puget Sound create strong westerly flow across a considerable part of the mountain chain. According to the model, this event occurring simultaneously with the approach of a 500-mb. ridge from the west, is ideal for the establishment of a stationary thermal ridge on the lee slopes.

GENERAL CASE

A general approach was utilized to study lee cyclogenesis. All instances of thermal ridge intensification on the lee slopes of the Rocky Mountains were systematically

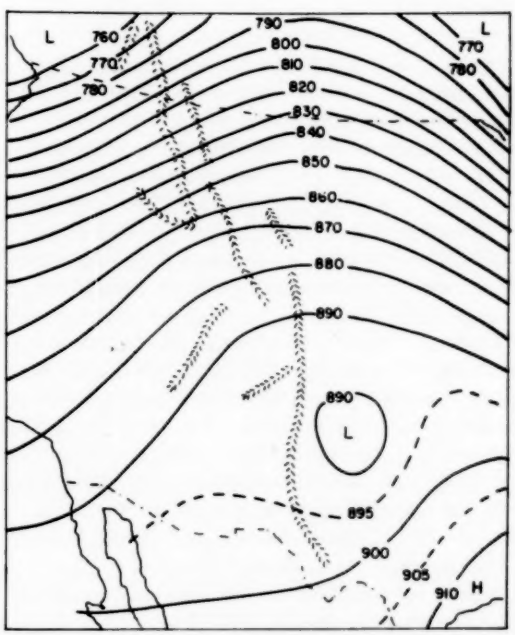

FIGURE 9.—500-mb. height contours (ft.), 0000 GMT, January 13, 1959 (ten of thousands and unit digits omitted).

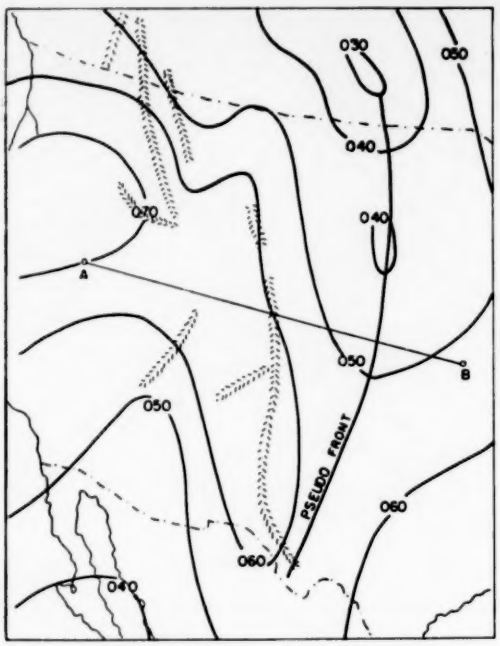

FIGURE 10.—1000-mb. height contours (ft.), 1200 GMT, January 13, 1959. A–B is position of atmospheric cross-section represented in figure 2 (unit digits omitted).

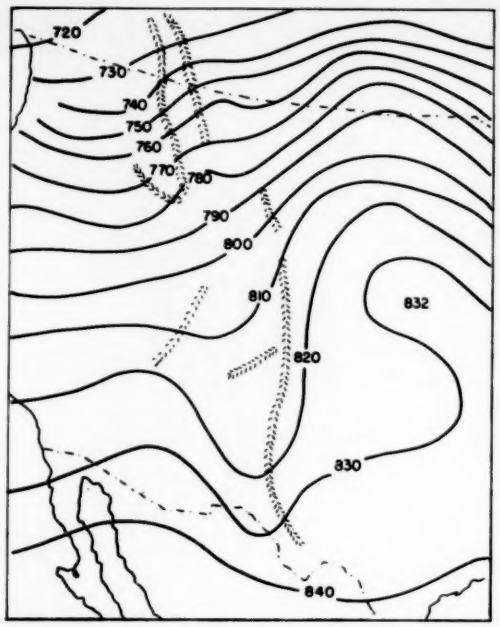

FIGURE 11.—1000–500-mb. thickness contours (ft.), 1200 GMT, January 13, 1959 (ten of thousands and unit digits omitted).

tabulated over the months December through March 1958–59 and 1959–60. The classification of the ridges was divided into two categories, "stationary" and "moving". The decision concerning the category of motion was qualitative, and based upon whether the thermal ridge appreciably moved eastward during the following 12-hour map interval.[2] Thermal ridges which remained stationary on more than one successive map were tabulated as "stationary" more than once. If the ridge later began to move eastward, it was tabulated again as "moving." For each case the position of the 500-mb. ridge and trough, relative to the thermal ridge, was tabulated. The results of this undertaking are presented in figure 13. The outstanding feature is the shift of the mean position of the 500-mb. ridge in the "stationary" cases to the east of the thermal ridge in the "moving" ones. Similarly, the mean position of the 500-mb. trough is situated at a distance greater than 15° of latitude west of the "stationary" thermal ridges, and about 12° west of the "moving" ones. The mean direction of the 500-mb. wind across the axis of the thermal ridge was 290° for the "stationary" cases and 265° in cases of "moving" thermal ridges. In all of the cases of thermal ridge development and motion (about 55), only four instances were accompanied by no definite trough-ridge pattern at 500 mb. The importance

[2] The surface map was always categorized before the 500-mb. flow was observed and categorized.

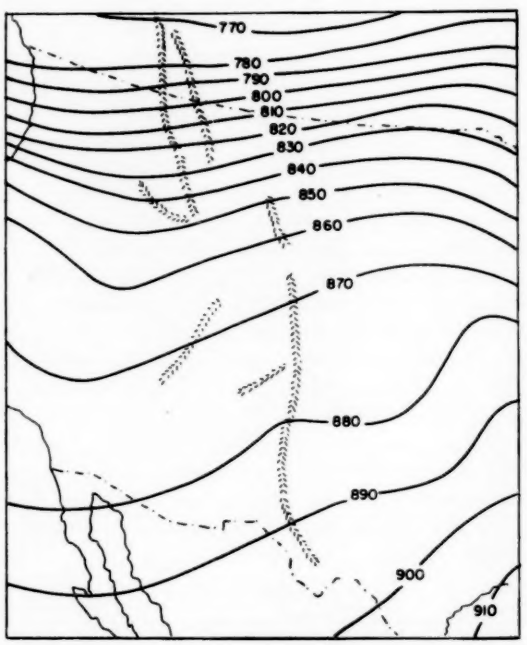

FIGURE 12.—500-mb. height contours (ft.), 1200 GMT, January 13, 1959 (ten of thousands and unit digits omitted).

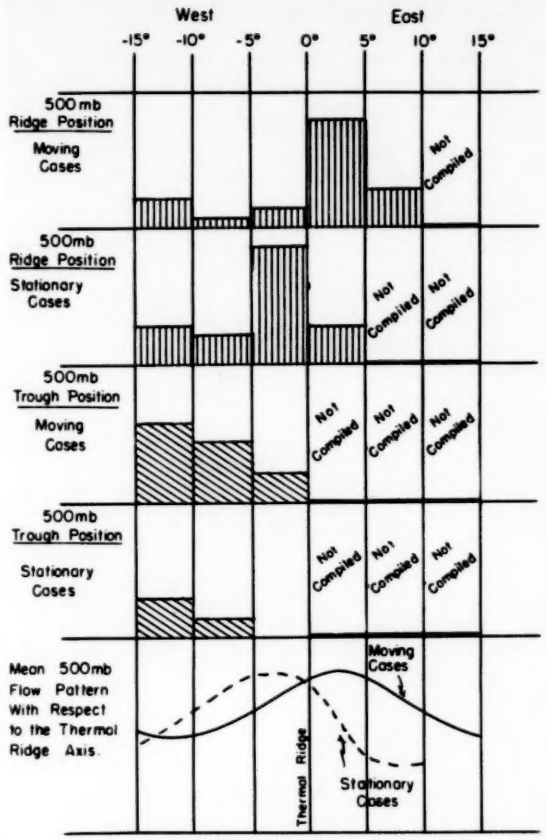

FIGURE 13.—Occurrence of 500-mb. troughs and ridges in 5° latitude intervals with respect to the thermal ridge axis, for stationary and moving cases. Compiled for the winters of 1958–59 and 1959–60 (units of ordinate go from 0 to 12 cases).

of the 500-mb. ridge in influencing the motion of lee-side disturbances is expressed by the term Q' in the numerator of equation (31). As the 500-mb. ridge approaches the lee slopes of the mountains, not only are conditions favorable for the initial development of thermal ridges, but those ridges which form will remain stationary for a short time due to the increasing effect of Q' which offsets the tendency for the thermal ridge to be advected downstream. Figure 13 also suggests that in the vicinity of 500-mb. troughs the numerator of (31) becomes vanishingly small, preventing the formation of thermal ridges.

5. SUMMARY AND CONCLUSIONS

The ultimate purpose of this paper was to study the development and motion of the frequently observed lower tropospheric frontogenesis associated with thermal ridge intensification on the lee slopes of the Rocky Mountains. The dynamical formulation showed that changes in the thermal pattern can be described by a potential thermal vorticity equation, which consists of three terms: (1) a term representing the advection of the potential thermal vorticity by the mean wind; (2) an orographic term; and (3) a term representing the advection of absolute vorticity at the mean level by the thermal wind. The mean level was considered to be 500 mb. An idealized sinusoidal model of the thermal ridge was devised in order to demonstrate the effect of each of the three terms on its motion. The results showed that the orographic effect was likely responsible for the thermal ridge amplification on the lee slopes of the mountains. According to the idealized pattern, the thermal ridge remains approximately stationary downstream from the point of maximum descent during the intensification process. Its amplitude continues to intensify until it attains a maximum critical value. At this point, the advection of potential thermal vorticity by the zonal flow at 500 mb. begins to dominate the motion, and the thermal ridge accelerates eastward. The effects of the perturbation in the 500-mb. current were shown to highly influence the development and motion of thermal ridges. The presence of migratory troughs and ridges at 500 mb. either (1) increases the maximum critical amplitude for stationarity, and thus increases the length of time for development, or (2) decreases the maximum critical amplitude, and therefore removes the stationarity condition, or (3) prevents any localized lee-slope thermal amplification from occurring.

An actual case was chosen to examine the development and motion of a thermal ridge in terms of the dynamical considerations. This undertaking provided a link between the theory and actual synoptic experience.

A survey of many cases was taken over the period of two winters. The results presented support the theory. Almost every case selected, whether it was stationary or moving eastward, was associated with a ridge at 500 mb. In the moving cases the 500-mb. ridge was generally centered east of the thermal ridge, and in the stationary instances it was centered west of the thermal ridge. Combined with the theory, these results lead to some conclusions concerning the nature of pseudo front development and motion.

The forecaster should consider the following criteria: (1) The thermal ridge will develop when the surface flow is such as to produce large-scale descent on the lee slopes of the mountains. (2) No thermal ridging will take place when the 500-mb. ridge lies downstream from lee slopes. (3) Thermal ridging will appear with the approach of a 500-mb. ridge from the west, and (4) will move eastward upon the passage of the 500-mb. ridge.

ACKNOWLEDGMENTS

The author is grateful to Professor Frederick Sanders of the meteorological department for his patient guidance in both the research and preparation of this manuscript.

REFERENCES

1. S. Petterssen, *Weather Analysis and Forecasting*, vol. II, Second Edition, McGraw-Hill Book Co., Inc., 1956. (See pp. 174–187.)
2. E. P. McClain, "Some Effects of the Western Cordillera of North America on Cyclonic Activity," *Journal of Meteorology*, vol. 17, No. 2, Apr. 1960, pp. 104–115.
3. S. L. Hess and H. Wagner, "Atmospheric Waves in the Northwestern United States," *Journal of Meteorology*, vol. 5, No. 1, Feb. 1948, pp. 1–19.
4. F. Sanders, A. James Wagner, and T. N. Carlson, "Specification of Cloudiness and Precipitation by Multi-Level Dynamical Models," *Scientific Report No. 1*, on contract AF 19(604)–5491, Massachusetts Institute of Technology, September 1960.
5. D. Colson, "Air Flow Over a Mountain Barrier," *Transactions, American Geophysical Union*, vol. 30, No. 6, Dec. 1949, pp. 818–830.
6. C. W. Newton, "Mechanisms of Circulation Change During a Lee Cyclogenesis," *Journal of Meteorology*, vol. 13, No. 6, Dec. 1956, pp. 528–539.
7. H. S. Buch, "Hemispheric Wind Conditions During the Year 1950," *Final Report Pt. 2* on contract AF19(122)–153, Department of Meteorology, Massachusetts Institute of Technology, 1954.
8. J. S. Sawyer and F. H. Bushby, "A Baroclinic Model Atmosphere Suitable for Numerical Integration," *Journal of Meteorology*, vol. 10, No. 1, Feb. 1953, pp. 54–59.
9. R. C. Sutcliffe, "A Contribution to the Problem of Development," *Quarterly Journal of the Royal Meteorological Society*, vol. 73, 1947, pp. 370–383.

SOME ASPECTS OF THE THERMAL ENERGY EXCHANGE ON THE SOUTH POLAR SNOW FIELD AND ARCTIC ICE PACK[1]

KIRBY J. HANSON

Polar Meteorology Research Project, U.S. Weather Bureau, Washington, D.C.

[Manuscript received September 13, 1960; revised February 21, 1961]

ABSTRACT

Solar and terrestrial radiation measurements that were obtained at Amundsen-Scott (South Pole) Station and on Ice Island (Bravo) T–3 are presented for representative summer and winter months. Of the South Polar net radiation loss during April 1958, approximately 20 percent of the energy came from the snow and 80 percent from the air. The actual atmospheric cooling rate during that period was only about 1/6 of the suggested radiative cooling rate. The annual net radiation at various places in Antarctica is presented. During 1958, the South Polar atmosphere transmitted about 73 percent of the annual extraterrestrial radiation, while at T–3 the Arctic atmosphere transmitted about 56 percent. The albedo of melting sea ice is discussed. Measurements on T–3 during July 1958 indicate that the net radiation is positive on both clear and overcast days but greatest on overcast days. Refreezing of the surface with clear skies, as observed by Untersteiner and Badgley, is discussed.

1. INTRODUCTION

The elliptical orbit of the earth brings it about 3 million miles farther from the sun at aphelion than at perihelion; consequently, during midsummer, about 7 percent less solar radiation impinges on the top of the Arctic atmosphere than on the Antarctic atmosphere during a comparable period. This difference is enhanced as solar energy penetrates into both polar atmospheres. Absorption, scattering, and reflection of the solar rays gives each polar region its own particular radiation environment. There are also other notable differences between the heat budgets of these two areas; for example, the conduction of heat through the ice is distinctly different. Annually, heat from the Arctic Ocean is conducted upward through the thin ice pack to the relatively cold surface where the temperature averages about −20° C. In contrast, the flux of heat through the ice layers of central Antarctica is quite small. Because of the heat budget differences, the annual temperature near the North Pole is about 30° C. warmer than that at the South Pole. It is the purpose of this paper to discuss some aspects of the thermal energy budgets of these regions.

The data which are presented were obtained during the International Geophysical Year and later years at Amundsen-Scott Station, located within a mile of the geographic South Pole, and at Ice Island T–3, drifting in the Arctic Ocean. This Island was about 5 by 11 miles in size and about 52 meters thick (Crary et al. [2]) in 1953 when it drifted near 88° N., 100° W. In the years that followed, this it drifted southward and in July 1958 was located 79.5° N., 118° W.

Solar radiation measurements at both stations were obtained with Eppley pyranometers. The data are corrected for the temperature response of the instrument (MacDonald [11]) and are presented in the International Pyrheliometric Scale of 1956. At both stations, Beckman and Whitley (Gier and Dunkle type) radiometers were used to measure the combined solar and terrestrial radiation streams.

2. WINTER MONTH AT THE SOUTH POLE

With the exception of a few weeks of twilight, sunset at the time of the March equinox marks the beginning of 6 months of continuous darkness at the South Pole. During the first of the dark months, April, the temperature a few meters above the snow averaged −58° C. (1957–59)—the same as the average temperature during the entire dark period.

In April 1958 the long-wave radiation[2] from the snow surface averaged 229 ly. day^{-1} (table 1), while the atmospheric (back) radiation returned 76 percent of this energy (175 ly. day^{-1}) to the surface. The net radiation averaged −54 ly. day^{-1}.

[1] Paper presented at the International Antarctic Symposium at Buenos Aires, November 1959.

[2] Terrestrial radiation, with most of the energy between wavelengths of 3 to 30 microns.

TABLE 1.—*Thermal energy exchange at the snow surface, Amundsen-Scott (South Pole) Station, Antarctica*

	January 1958	April 1958	Annual 1958
Incident solar radiation (ly. day^{-1})*	770	0	266
Reflected solar radiation (ly. day^{-1})	674	0	218
Albedo (percent)	88		82
Snow surface radiation (ly. day^{-1})	440	229	301
Atmospheric (back) radiation (ly. day^{-1})	309	175	218
Return (percent)	70	76	72
Net radiation (ly. day^{-1})	−35	−54	−35
Thermal energy from snow (ly. day^{-1})		11	
Thermal energy from air (ly. day^{-1})		43	

*One Langley (ly.) equals one cal. cm.$^{-2}$

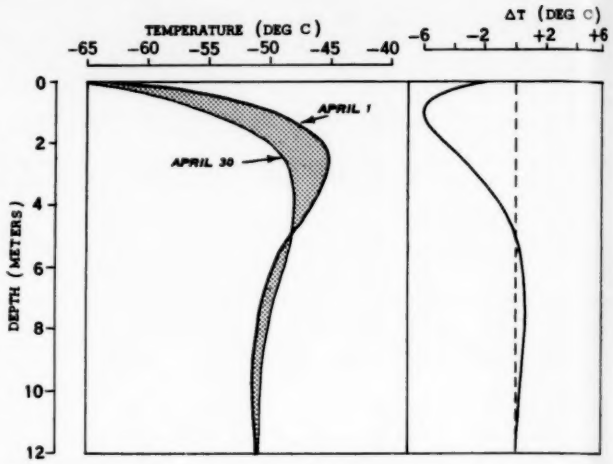

FIGURE 1.—Snow temperature profiles of April 1 and 30, 1958, and monthly temperature-change profile, Amundsen-Scott (South Pole) Station, Antarctica.

The total thermal energy in the top 12 meters of snow at the beginning and end of April 1958 was calculated, using the equation

$$Q=\int_0^{12} c\rho T dz \qquad (1)$$

where c is the specific heat in cal. gm^{-1} deg.$^{-1}$ (List [9]), ρ is the density in gm. cm.$^{-3}$ (Giovinetto [4]), and T is the temperature (fig. 1) in °K. The calculations indicate that during the month heat was conducted to the surface at the rate of 11 ly. day^{-1}. This suggests that, of the net radiation loss during April, about 20 percent of the energy came from the snow and 80 percent from the air. During clear, cold periods at the South Pole the snow and air supply about equal amounts of energy to make up the surface radiation loss (Hanson [6]). Liljequist [8] found that with clear skies at Maudheim, along the coast of Antarctica, roughly 40 percent of the required energy comes from the snow and 60 percent from the air.

Some idea of the heat budget of the atmosphere during this period can be obtained from the airborne radiation measurements which were taken with Suomi airborne radiometers (Suomi et al. [14]). Data from the clear-sky flight on April 27, 1959 (fig. 2) indicate a radiative loss of 240 ly. day^{-1} at 50 mb. Assuming this loss is representative of April 1958, and adding the small amount of heat which was conducted from the snow (11 ly. day^{-1}), the net cooling rate from the surface to 50 mb. becomes 1.49° C. day^{-1}. This is about 6 times greater than the observed cooling rate (0.26°C. day^{-1}). Presumably, subsidence and advection provide the necessary energy to account for the discrepancy.

3. SUMMER MONTH AT THE SOUTH POLE

Even though the South Polar plateau receives more solar radiation at midsummer than any other area on earth, the temperature of the snow surface remains well below freezing. In January, the warmest month of the summer, the temperature averages near −27° C., and rarely exceeds about −17° C.

During January 1958, with continuous sunlight at the South Pole, the incoming solar (sun and sky) radiation averaged 770 ly. day^{-1}. Measurements indicate that, of this amount, 88 percent (674 ly. day^{-1}) was reflected from the snow, while the remainder (96 ly. day^{-1}) was absorbed. During the same period, the snow surface radiated 440 ly. day^{-1}, while the atmospheric (back) radiation returned 70 percent (309 ly. day^{-1}) of that energy. The net radiation averaged −35 ly. day^{-1}.

4. ANNUAL ENERGY EXCHANGE, ANTARCTICA

During the 6 months of sunlight at the South Pole, the solar radiation which was incident on the snow totaled 9.71×10^4 ly. The snow reflected 7.96×10^4 ly., indicating an average albedo of 82 percent for the sunlit period.

Unlike solar radiation, the emission of long-wave radiation by the snow is continuous throughout the year. During 1958, the snow surface radiation averaged 301 ly. day^{-1}, of which about 72 percent (218 ly. day^{-1}) was returned by atmospheric (back) radiation. This percentage is relatively unchanged from summer to winter even though the sky is much clearer during winter (fig. 3). With other things being equal, clear skies would certainly tend to lower this percentage. Apparently, a compensating factor is that the surface temperature inversion is more intense during winter; this would allow a greater return of the surface radiation.

The net radiation at the South Pole (2800 m.) averaged about −35 ly. day^{-1} during 1958. Liljequist [7] found an annual loss of 25 ly. day^{-1} at Maudheim, and Loewe [9] found a loss of 20 ly. day^{-1} at Port Martin. Both stations are located along the coast of Antarctica. Rusin [13] has reported an annual net radiation of −6 to −8 ly. day^{-1} at Mirny, another coastal station, and −19 to −22 ly. day^{-1}

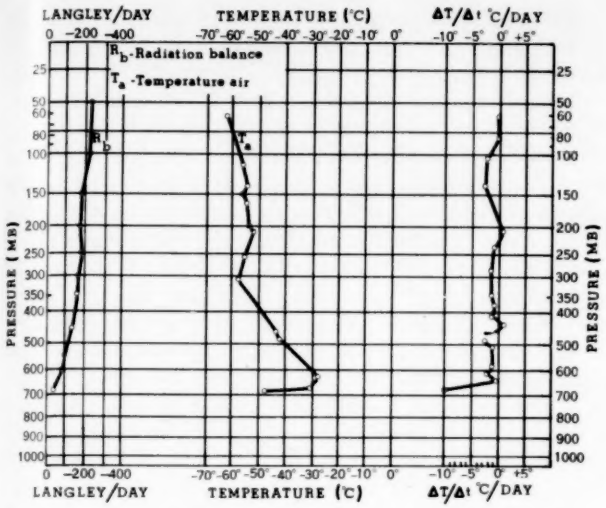

FIGURE 2.—Net radiation profile, temperature profile, and temperature-change profile computed from radiometersonde (Suomi et al. [14]) ascent at Amundsen-Scott (South Pole) Station, Antarctica, 0600 GMT April 27, 1959.

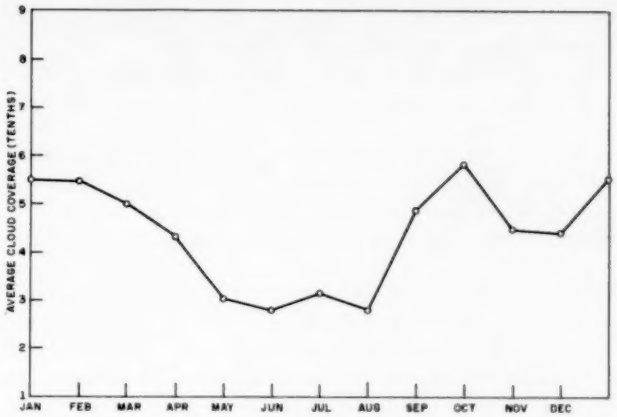

FIGURE 3.—Average cloud coverage during the period January 1957 through December 1960 at Amundsen-Scott (South Pole) Station, Antarctica.

at Pionerskaya (2700 m.) in the interior of eastern Antarctica. There is little doubt that, as a whole, the surface of Antarctica has a negative net radiation, although certain snow-free areas on the continent and portions of the Palmer Peninsula are probably positive. Considering the magnitude of the individual incoming and outgoing radiation streams, the slight variation of net radiation, as observed in Antarctica, seems rather remarkable.

5. ANNUAL ENERGY EXCHANGE, ARCTIC OCEAN BASIN

Although the elliptical orbit of the earth causes comparatively less midsummer extraterrestrial radiation in the Arctic, it also provides 9 additional days of sunlight at the North Pole each year compared to the South Pole. The net result is that during the course of their respective sunlit periods, equal amounts of solar energy impinge on the top of the North and South Polar atmospheres. This was pointed out by Milankovitch [12], who indicated that at both geographic poles the annual extraterrestrial radiation is of equal intensity, and, assuming a solar constant of 2.00 ly. min.$^{-1}$, totals 13.33×10^4 ly. during the year. This equality is not maintained as the solar rays penetrate the polar atmospheres, however. The previously mentioned measurements at the South Pole indicate that, annually, about 73 percent of the extraterrestrial radiation was incident on the snow surface. At Ice Island T–3, on the other hand, only about 56 percent of the extraterrestrial radiation [3] was incident at the surface during 1958.

[3] Located at 79.5° N., the extraterrestrial radiation at T–3 totaled 13.81×10^4 ly. during 1958.

The fact that a smaller percentage of the extraterrestrial radiation reaches the surface in the Arctic may be due to a number of factors: possibly there are thicker cloud systems in the Arctic, the surface albedo is less in the Arctic, and the optical thickness of the Arctic atmosphere is greater because of the comparatively lower surface elevation of the Arctic. Precisely how these variables affect the amount of solar energy, incident on the Arctic and Antarctic, is difficult to determine without a better knowledge of the surface albedo and thickness of the cloud systems (Fritz [3]).

6. SUMMER MONTHS IN THE ARCTIC

The snow that covers much of the Arctic sea-ice in early spring is gradually melted during May and June. As a result, pools of melt water form on the ice floes in late June and remain during July and sometimes August. These pools aid in lowering the surface albedo during this midsummer ablation period. Sverdrup [15] has indicated that the albedo of melting Arctic sea-ice is between 60 and 65 percent. Recent Soviet investigations (Briazgin [1]) have shown a similar albedo value, 60 percent. The fact that pools of melt water on the floes lower the albedo is indicated by the results of an aerial albedo survey over the Arctic Ocean. This survey indicated that the albedo of melting ice with a maximum amount of puddling is about 46 percent (Hanson [5]).

Measurements on T–3 indicate that during July 1958 the incident solar radiation averaged 524 ly. day^{-1}. Assuming an albedo of 60 percent, the ice would have gained 210 ly. day^{-1}. Measurements also indicate that, with an average 6.7-tenths cloud coverage, the atmospheric long-wave radiation returned about 88 percent (578 ly. day^{-1}) of the 653 ly. day^{-1} which were emitted as long-

wave radiation from the surface. This gives an average net radiation of +135 ly. day^{-1} during July.

Currently, one of the most important questions in polar heat-budget investigations is: How is the "surplus" thermal energy, available from radiative exchange, used in warming or melting the ice, evaporation, or warming the lower atmosphere? During the previously mentioned period, for example, the net radiation could have melted 58 cm. of surface ice, assuming a density of 0.9 gm. cm.$^{-3}$ and a latent heat of fusion of 80 cal. gm.$^{-1}$ The actual ablation was probably somewhat less, however, as a small amount of energy is lost in evaporation (Untersteiner and Badgley [16]), and possibly, as Fritz [3] and Yakovlev [17] have suggested, some energy may be lost to the atmosphere by turbulence. Because ablation, evaporation, and temperature profile measurements are not available, the heat and water budget during this important summer ablation period cannot be determined precisely.

An interesting observation regarding the heat budget was made by Untersteiner and Badgley [16] on Floating Ice Station "A":

> During the summer, melting occurred mostly when there was overcast and strong atmospheric radiation. Radiosonde observations reveal frequent inversions, with comparatively high cloud temperatures. Temporary breaks in the overcast were frequently accompanied by freezing at the surface even though direct solar radiation was relatively larger in such periods.

In order to investigate the role of radiative heat in melting, we have examined the radiation data for clear and overcast conditions at T-3 during July 1958. From measurements of the incoming solar and atmospheric (back) radiation, assuming an albedo of 60 percent which is probably representative of the melting pack ice, it was found (table 2) that on 6 clear days the net radiation averaged +76 1y. day^{-1}. On 9 overcast days it averaged +147 1y. day^{-1}—an increase by a factor of about 2 providing the albedo is unchanged. The radiation data, as presented here, lend some support in explaining these observations made by Untersteiner and Badgley [16]. However, a full explanation would require some idea of the rates of evaporation and turbulent heat exchange in the boundary layer.

There is also an additional point of interest. In view of the observed refreezing of the surface with clear skies, it is rather surprising that the net radiation should be positive. An examination of the data revealed that an albedo of 72 percent or higher would be required in order to have a negative net radiation with clear skies. This seems excessive. It seems reasonable that if freezing of the surface occurs with a positive radiation balance, either one of two things is happening. Either the total heat budget is *negative* because of losses by evaporation and turbulence and therefore refreezing of the surface occurs; or, the total heat budget is *positive* and the "surplus" energy is used in melting just below the surface while freezing continues on the surface. The latter may be possible as the ice is partially transparent to solar radiation and opaque to the longer wavelengths of terrestrial origin. In order to present a realistic model of the processes involved, additional field studies are desirable.

TABLE 2.—*Thermal energy exchange at the surface of Arctic sea-ice during clear, overcast, and average sky conditions as determined from measurements of incident solar and atmospheric (back) radiation at T-3, assuming an albedo of 60 percent and ice surface temperature of 0° C.*

	July 1958		
	Clear sky condition, ≤1-tenth sky cover (on 6 days)	Overcast sky condition, 10-tenths sky cover (on 9 days)	Average sky condition, 6.7-tenths sky cover (31 days)
Incident solar radiation (1y. day^{-1})	643	401	524
Reflected solar radiation (assuming an albedo of 60 percent) (1y. day^{-1})	386	241	314
Ice surface radiation (1y. day^{-1})	653	653	653
Atmospheric (back) radiation (1y. day^{-1})	472	640	578
Return (percent)	72	98	88
Net radiation (1y. day^{-1})	+76	+147	+135

ACKNOWLEDGMENTS

The writer gratefully acknowledges the many helpful comments from Drs. H. Wexler and S. Fritz. This work was made possible by support from the National Science Foundation of the National Academy of Sciences.

REFERENCES

1. N. N. Briazgin, "K Voprosu ob Al'bedo Poverkhnosti dreĭfuûshchikh l'dov," [On the Question of the Albedo on the Surface of Drifting Ice], *Problemy Arktiki, i Antarktiki* No. 1, 1959, pp. 33–39.
2. A. P. Crary, J. L. Kulp, and E. W. Marshall, "Evidences of Climatic Change from Ice Island Studies," *Science*, vol. 122, 1955, pp. 1171–1173.
3. S. Fritz, "Solar Radiation Measurements in the Arctic Ocean," pp. 159–166 of *Proceedings, Polar Atmosphere Symposium, Oslo, July 1956, Part I, Meteorology Section*, Pergamon Press, New York, 1958.
4. M. Giovinetto, Unpublished document, 1958. (Presents measurements of snow density from the surface to −12 meters for the South Pole.)
5. K. J. Hanson, "The Albedo of Sea Ice and Ice Islands in the Arctic Ocean Basin," 1960.
6. K. J. Hanson, "Radiation Measurement on the Antarctic Snowfield, A Preliminary Report," *Journal of Geophysical Research*, vol. 65, No. 3, Mar. 1960, pp. 935–946.
7. G. H. Liljequist, "Energy Exchange of an Antarctic Snowfield, Long-Wave Radiation and Radiation Balance," *Norwegian-British-Swedish Antarctic Expedition, 1949–52, Scientific Results*, vol. II, Part IB, Oslo, 1956, pp. 113–183, (p. 174).
8. G. H. Liljequist, "Energy Exchange of an Antarctic Snowfield, Wind Structure in the Low Layer," *Norwegian-British-Swedish Antarctic Expedition, 1949–52, Scientific Results*, vol. II, Part 1C, Oslo, 1957, pp. 187–233, (p. 224).
9. R. J. List (ed.), *Smithsonian Meteorological Tables*, 6th revised edition, Smithsonian Institution, Washington, D.C. 1951, (see p. 343).
10. F. Loewe, "Études de Glaciologie en Terre Adélie, 1951–52,"

Expéditions Polaires Francaises, No. 9, *Actualités Scientifiques et Industrielles*, No. 1247, Hermann et Cie., Paris, 1956, 159 pp.

11. T. H. MacDonald, Unpublished document, 1959. (Presents the results of temperature response tests on the Eppley pyranometers which were used at United States stations in the Arctic and Antarctic during the International Geophysical Year.)
12. M. Milankovitch, "Mathematische Klimalehre," *Handbuch der Klimatologie*, W. Köppen und R. Geiger, Band I, Teil A, Berlin, 1930, (pp. A30–A31 and table 3).
13. N. P. Rusin, "Radiatsionnyĭ Balans Snezhnoĭ Poverkhnosti v Antarktide," [Radiation Balance of the Snow Cover in the Antarctic], *Informatsionnyĭ Bŭlleten' Sovetskoi Antarkticheskoĭ Expeditsiĭ*, No. 2, Leningrad, 1958, pp. 25–30.
14. V. E. Suomi, D. O. Staley, and P M. Kuhn, "A Direct Measurement of Infra-Red Radiation Divergence to 160 mb.," *Quarterly Journal of the Royal Meteorological Society*, vol. 84, No. 360, Apr. 1958, pp. 134–141.
15. H. U. Sverdrup, "Meteorology, Part I, Discussion," *The Norwegian North Polar Expedition with the "Maud", 1918–1925, Scientific Results*, vol. II, Geofysisk Institutt, Bergen, 1933, pp. 1–328.
16. N. Untersteiner and F. I. Badgley, "Preliminary Results of Thermal Budget Studies on Arctic Pack Ice During Summer and Autumn," pp. 85–95 of *Proceedings, Arctic Sea Ice Conference, Easton, Maryland, Feb. 24–28, 1958*, National Research Council, Washington, D.C., Publication No. 598, Dec. 1958.
17. G. N. Yakovlev, "Solar Radiation as the Chief Component of the Heat Balance of the Arctic Ice," pp. 181–189 of *Proceedings, Arctic Sea Ice Conference, Easton, Maryland, Feb. 24–28, 1958*, National Research Council, Washington, D.C. Publication No. 598, Dec. 1958.

THE WEATHER AND CIRCULATION OF FEBRUARY 1961[1]

An Example of Attentuation in the Long-Wave Pattern

L. P. STARK

Extended Forecast Section, U.S. Weather Bureau, Washington, D.C.

1. CONTRASTING REGIMES IN WINTER 1960–61

Attenuation of the long-wave features in the western portion of the Northern Hemisphere in February 1961 was in marked contrast to the patterns that had prevailed in the preceding winter months. In December [1] and January [2] pronounced amplification of the monthly mean 700-mb. flow pattern dominated the circulation and effectively controlled the weather in North America. Widespread cold conditions in December were repeated in January in the East and South in response to the strong ridge in western North America that extended from the Great Basin to the Arctic Ocean. Substantial changes in the circulation in February 1961 (fig. 1) produced strong damping of the long waves in the mid-troposphere. As a result the country was subjected to mild Pacific air masses instead of cold continental air; the westerlies at mid-latitudes over North America were strengthened; and temperatures in the East became warmer than normal near the end of the winter season.

2. SOME ASPECTS OF THE MONTHLY MEAN CIRCULATION

The changes in circulation from January to February are best examined by referring to figure 2, the difference in 700-mb. height departure from normal between the two months. The greatest changes were in the Pacific, where most of the area underwent height rises in February, and the deep, cyclonic center of January at middle latitudes weakened and moved northward. Consequently, the ridge in western North America could no longer be sustained in such strength as was noted in December and January. Heights fell throughout the area from January to February, with maximum change of −420 feet in the Yukon (fig. 2).

The trough in eastern North America advanced to the central Atlantic as flattening of the pattern progressed downstream. Height anomalies increased over most of eastern North America (maximum of +310 ft. in New York) where contour curvature changed from strongly cyclonic in January to slightly cyclonic in February. The result of these changes in and near North America was a decided increase in the average speed of the westerlies at mid-latitudes. The hemispheric zonal index (5° W.–175° E.) was 2 m.p.s. greater in February than it was in January. This increase occurred despite a regional decrease in westerlies from the central Atlantic to Europe where the meridional component of the flow dominated.

In western Europe changes in the average circulation at 700 mb. were large. Diffluent, cyclonic flow in January was replaced in February by a strong ridge (fig. 1) in which there were maximum height rises of 390 feet in Spain (fig. 2). The evolution of this ridge was simultaneous with damping of the pattern in the eastern Pacific and western North America; its growth deserves further comment, based on 5-day mean 700-mb. charts one week apart (not shown).

On the 5-day mean chart for February 2–6, a high center was located just to the west of Morocco with a flat ridge extending northward to Scotland. One week later the High was centered over Gibraltar and the ridge was still rather flat to the north, but the trough southward from Greenland had become quite deep near 40° N. Meanwhile a positive height anomaly center of 390 feet had moved from Gibraltar to northern Spain and increased to 590 feet.

During the week of February 16–20 the anomaly center reached a maximum of 760 feet above normal in France and was associated with a dominant blocking High. In the last week of February the High was observed over the Baltic Sea, still strong, with an omega-configuration well defined by a strong trough (negatively tilted) in the eastern Atlantic and a deep resonant trough from northwestern Siberia to the Red Sea.

Another blocking High was observed on the 30-day mean chart (fig. 1) over northeastern Siberia, but this was considerably weaker than the one in Europe. Its development occurred as the trough along the Asian coast deepened at middle and low latitudes and as the ridge which was in the Arctic Ocean in January retrograded.

[1] The weather of March, April, and May 1961 will be described in the June, July, and August 1961 issues of the Review, respectively.

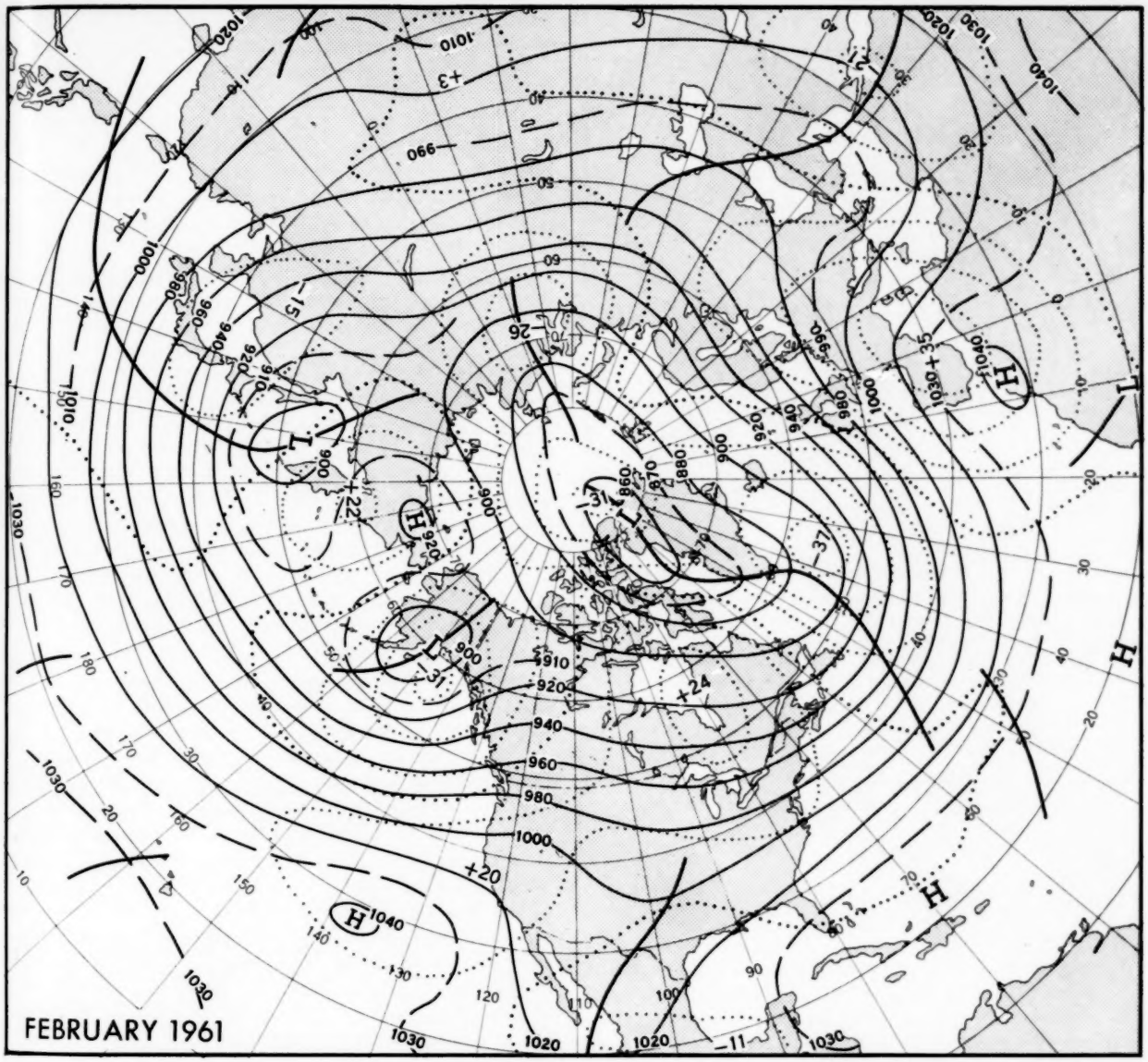

FIGURE 1.—Mean 700-mb. contours (solid) and departures from normal (dotted), both in tens of feet, for February 1961. The trough in the Southwest intensified as the wavelength and westerlies increased at mid-latitudes.

Ordinarily the effect of blocking shows up in a migration southward of the westerlies and a decrease in the average zonal wind speed. But the blocking Highs this month were too far removed to have an appreciable effect on the zonal index in the western portion of the Northern Hemisphere or on the weather and circulation in North America. Dominant in the weather of the United States were the generally westerly flow from the eastern Pacific to the western Atlantic, and especially, the position of the Aleutian Low at an extreme northeast location.

3. WEATHER RELATED TO THE MEAN CIRCULATION

TEMPERATURE

Departures of average surface temperature from normal (fig. 3) were predominantly positive except for a small area in the Southwest where it was 1°–2° F. cooler than normal. The correspondence was close between the flow pattern and the temperature anomaly. Compare the height departure from normal (dotted lines fig. 1) with the temperature departures in figure 3. Considering

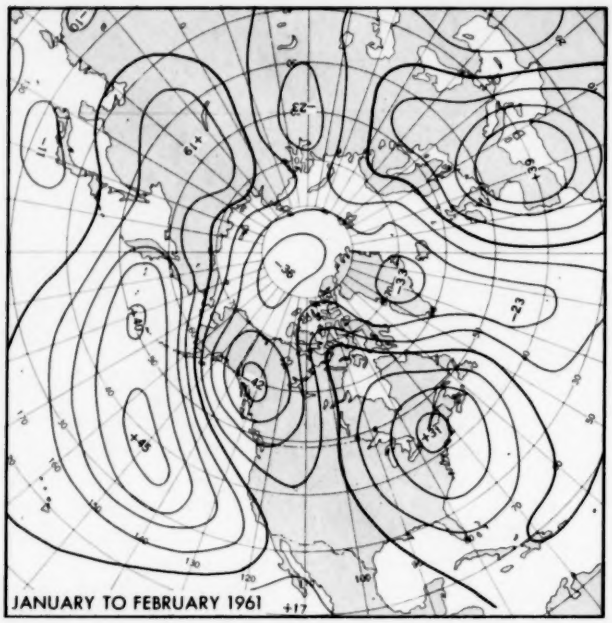

FIGURE 2.—Change of mean 700-mb. height departures from normal (tens of feet) from January 1961 to February 1961. Attenuation of flow pattern near North America in February is accented by falls in the ridge in western North America and rises in the troughs in the eastern Pacific and western Atlantic.

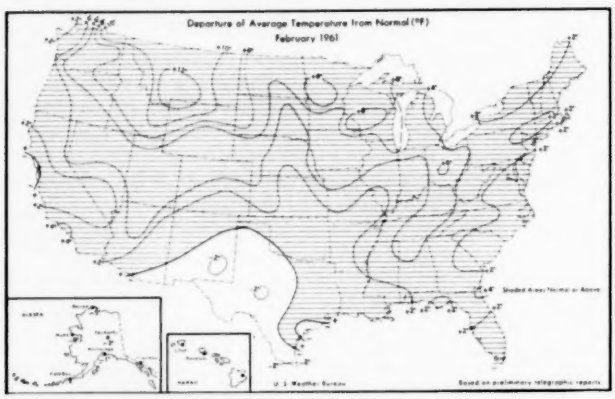

FIGURE 3.—Departure of average temperature from normal (°F.) for February 1961. Height anomaly (fig. 1) and temperature anomaly are almost identical in pattern. (From [5].)

sign only, the similarity in the patterns is remarkable; considering magnitude, the analogy is weaker.

The correlation between local 700-mb. heights and surface temperature anomaly is generally positive, but average correlations in the winter months explain only about 35 percent of the temperature variance [3]. By statistically integrating the behavior of the atmosphere at various distances from the local area, the explained variance can be considerably increased [4]. The synoptic

TABLE 1.—*Class changes of monthly average surface temperature anomalies in 100 cities from January to February 1961*

Class change*	Frequency (percent)
+4	0
+3	21
+2	23
+1	30
0	19
−1	7
−2	0
−3	0
−4	0

*+indicates a change toward higher average temperature. Classes are much below normal, below normal, near normal, above normal, and much above normal.

interpretation of this statistical result is dependent on the well-known fact that the position of the Aleutian Low has a controlling effect on temperatures in much of North America. In February it is normally located over Kamchatka. When it is displaced far to the east (as it was in February 1961), 700-mb. heights are usually lower than normal in northwestern North America (as they were this month)(fig. 1). The resulting westerly flow prevents outbreaks of Arctic air from penetrating into latitudes below 40° or 50° N. Furthermore, increased westerlies at these latitudes in the eastern Pacific (4–8 m.p.s. stronger than normal this February) undergo strong katabatic warming after striking the middle Rockies. The total effect is frequently unseasonable warmth east of the Divide at middle latitudes.

The change in temperature regime from January to February was determined by the circulation change (fig. 2). Consequently, persistence of temperature was large west of the Mississippi River, where height changes were small; to the east, temperatures changed radically where height changes were relatively large. A summary of the January to February changes in monthly average temperature (in terms of five classes) at 100 cities (table 1) indicates the following: (a) 74 percent of the temperatures became warmer, (b) 7 percent became cooler, and (c) 21 percent became warmer by three classes (from much below normal to above normal).

PRECIPITATION

Precipitation in February (fig. 4) was much more extensive and generally heavier (in 64 of 100 cities) than it was in January [5]. From the Ohio Valley to the western Plateau and from the Canadian border to the Southern Plains, little or no precipitation fell in January, when northerly flow at 700 mb. and sea level inhibited the transport of moist air masses into the country. In February the average flow aloft (fig. 1) and at sea level [6] encouraged the advection of moisture northward from the Gulf of Mexico and eastward from the Pacific.

In the Pacific Northwest there was a deep onshore flow from sea level to 700 mb. This current, the core of maximum wind speed or "jet stream" at 700 mb., supported a very high frequency of frontal systems, 8 to 12

crossing the coast in February. As much as 20 in. of rain fell along the Washington coast as moist, Pacific air was forced to ascend the mountain slopes. Precipitation records for February were broken at Olympia, Wash. (7.02 in. above normal), Sexton Summit, Oreg. (6.75 in. above normal), and several other stations in Washington and Oregon. Flooding was reported in the Puget Sound area, the Olympic Peninsula, and the Willamette Basin.

In the Southeast the distribution of precipitation was related almost ideally to the 700-mb. pattern [7]. Heavy precipitation occurred in the southwesterly flow ahead of the trough and through the weak ridge (fig. 1). There was additional support from the southeasterly anomalous component of the 700-mb. flow and from the warm, moist air at sea level that had a long trajectory from the Tropics. Locally severe flooding from Mississippi to Georgia resulted from 8 in. to more than 17 in. of precipitation that fell in a narrow band from Louisiana to western South Carolina (fig. 4). Several cities in Alabama and Georgia reported the wettest February of record. From early reports precipitation was heaviest in Birmingham and vicinity, where the total was 17.67 in., 12.50 in. greater than normal.

In contrast to the wet weather just described were continued drought conditions over most of the Southwest. Many cities had near-record dryness for February and for the winter season. At Cheyenne, Wyo., and Grand Junction, Colo., February was the 16th and 11th consecutive month, respectively, in which precipitation was less than normal. A deficit of precipitation in February contributed to the driest winter of record at Chicago, Ill., Lansing, Mich., and Burbank, Calif.

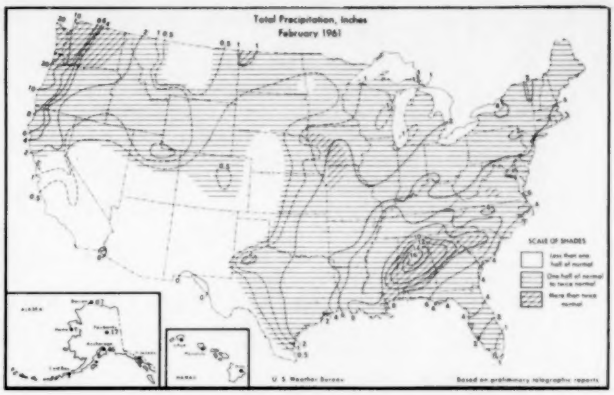

FIGURE 4.—Total precipitation, inches, for February 1961. Locally severe flooding in the Northwest and in the Southeast was closely related to strong southwesterly flow in advance of mean troughs. (From [5].)

4. INTRA-MONTHLY TRANSITION

JANUARY 31–FEBRUARY 14

The 700-mb. circulation in the first half of February (fig. 5A) was transitional between the large-amplitude circulation of January and the higher index state during the last half of February.

In the eastern Pacific, despite appreciable filling, the eastern lobe of the Aleutian Low was still rather strong. The sea level counterpart (fig. 5B) was 11 mb. below normal, as intense as any vortex on the chart, but considerably weaker than the same Low in January, when pressures for the month averaged 20 mb. below normal [2].

The ridge over North America had much less amplitude than in January and was somewhat farther east. Height falls at 700 mb. eroded the western portion of the ridge at middle and high latitudes as the center of positive height departure from normal jumped from British Columbia in January to Hudson Bay in the first half of February.

In the Atlantic the strong trough at 700 mb. progressed from the east coast and deepened as cold air was injected from Canada. The Icelandic Low at sea level was near its normal position, but was 11 mb. deeper than normal.

The distribution of temperature departures from normal for January 31–February 14 is shown in figure 5C. From the Central Plains westward, temperatures ranged from 4°–18° F. warmer than normal. Most of this warmth was a function of the ridge aloft; some was related to the increasing westerlies and the deep Low in the Gulf of Alaska. In the eastern portions of the country cold air was closely associated with the anomalous northerly components of the flow at 700 mb. and at sea level. The source and trajectory of the cold air observed in the East was implicit in the strong ridge at sea level from Hudson Bay to the Gulf Coast (fig. 5B).

FEBRUARY 15–MARCH 1

During the last half of February broadscale damping of the major perturbations occurred in mid-latitudes from the central Pacific to the eastern Atlantic (fig. 6A). The Aleutian Low continued to weaken as heights increased as much as 480 feet in the eastern Pacific. At the same time heights decreased over Canada, and cyclonic flow prevailed from Alberta to Labrador, in place of the ridge formerly there. In the western Atlantic height rises were widespread and reached a maximum of 390 feet where there had been a trough the first half of the month. This nearly simultaneous growth of the Bermuda High and the High in the eastern Pacific suggests a teleconnection often noted in a period of rising index.

General height falls in higher latitudes and rises in middle latitudes contributed to a pronounced strengthening of the zonal index in temperate latitudes. At midmonth the 5-day mean 700-mb. zonal index (5° W.–175° E.) was 10.5 m.p.s., only 0.3 m.p.s. above normal. By the end of February, however, the index had jumped to 13.6 m.p.s., 3.8 m.p.s. above normal.

Deepening of the trough in the lee of the Rockies was assisted by the increased westerlies impinging on this natural barrier. Accompanying the increased cyclonic

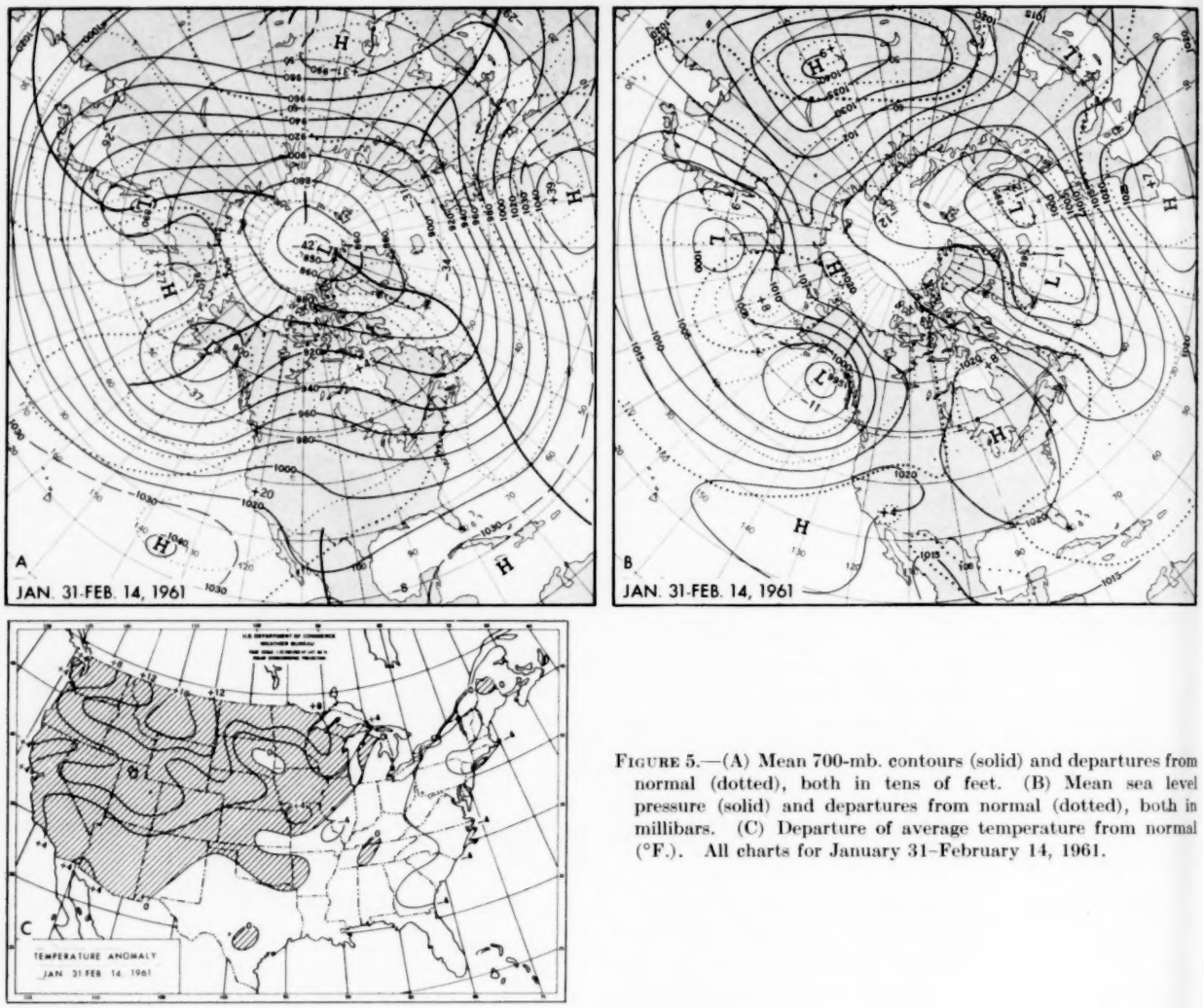

FIGURE 5.—(A) Mean 700-mb. contours (solid) and departures from normal (dotted), both in tens of feet. (B) Mean sea level pressure (solid) and departures from normal (dotted), both in millibars. (C) Departure of average temperature from normal (°F.). All charts for January 31–February 14, 1961.

flow were vigorous frontal systems that crossed the Rockies and intensified just to its lee. In fact, there were 16 days of frontal activity in Montana during the month, a maximum for the country.

The sea level chart for February 15–March 1 (fig. 6B) should be compared with that of the first half of February (fig. 5B). Changes indicated are similar to those found on the 700-mb. charts for the same periods. The complementary anticyclogeneses in the eastern Pacific and the western Atlantic are clearly portrayed by the dotted lines showing the sea level pressure departures from normal. In the same period sea level pressures fell 5–9 mb. from the Gulf of Mexico to Baffin Bay. The direction of the flow and its anomalous components are indicative of the changed regime. Note especially the northerly direction in the West and the southerly direction in the East.

A great warming in the East and a cooling in the West were the principal reactions to the reversed flow. Figure 6C shows that average temperatures for February 15–March 1 were generally 4°–8° F. warmer than normal over most of the country and a few degrees cooler in the Southwest. But the changes from the first half of February to the last half were quite large. In the East, for example, temperature anomalies showed positive changes of 12°–16° F. in a belt from Florida to New York; west of the Plains States negative changes ranged from 4°–10° F.

As the transition in the circulation proceeded, there was a definite change in the tracks of cyclones in and near North America. This might be anticipated from a study of figures 5 and 6, but for additional emphasis and clarity, figure 7 is presented. This figure was prepared by separating the tracks of migratory cyclones published in

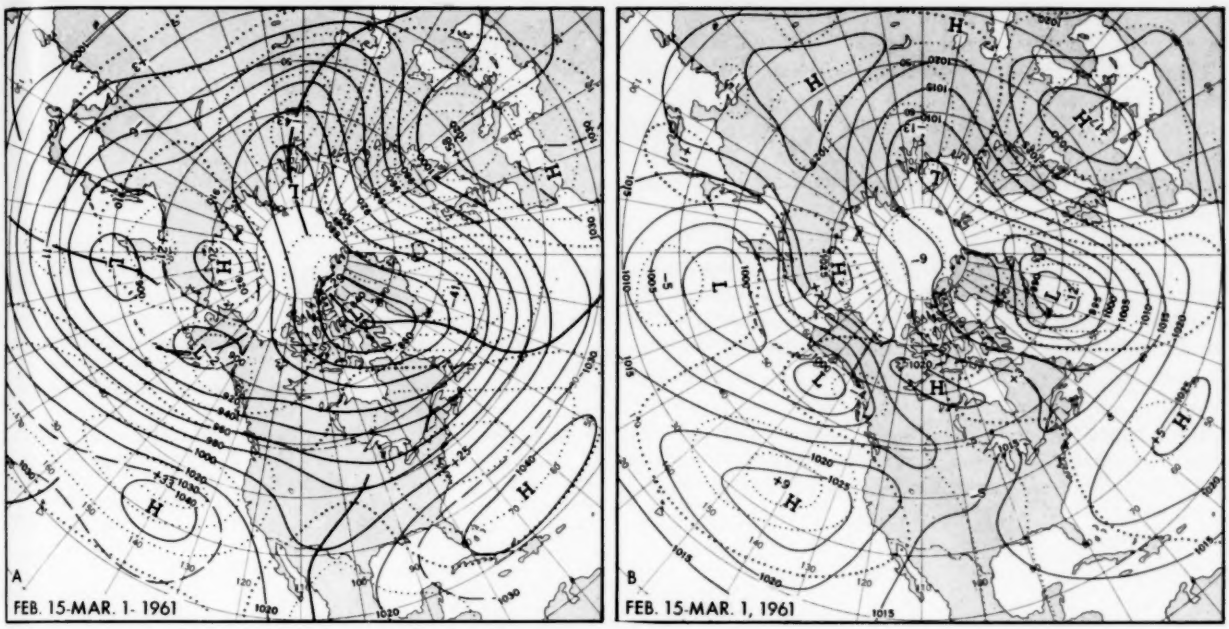

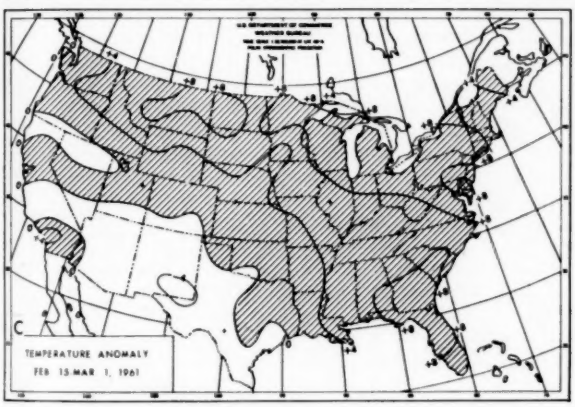

FIGURE 6.—(A) Mean 700-mb. contours (solid) and departures from normal (dotted), both in tens of feet. (B) Mean sea level pressure and departure from normal, both in millibars. (C) Departure of average temperature from normal. All charts for February 15–March 1, 1961.

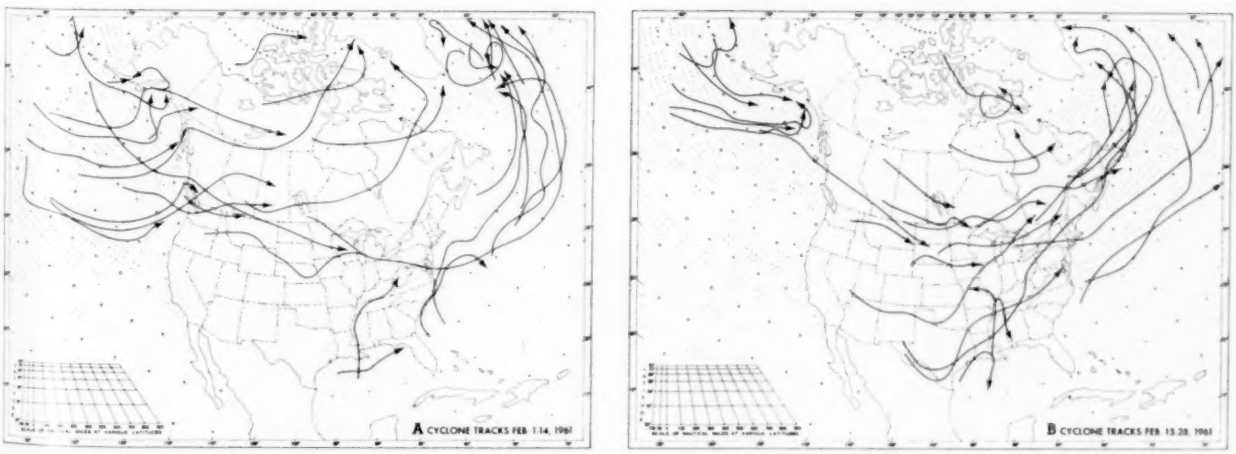

FIGURE 7.—Paths of migratory cyclones (A) Feb. 1–14, 1961, and (B) Feb. 15–28, 1961. Note general shift of cyclones northward in both oceans and increased frequency of tracks originating in the Southwest from the first half to the last half of February.

[6] into halves; those originating in the first half of February (A) and those originating in the second half (B).

These tracks clearly illustrate the changes discussed above. The transfer of cyclonic activity in the Pacific to a more northerly locus was a typical result of anticyclogenesis in the eastern Pacific. In the Atlantic the average storm track was displaced to the north in a similar manner for a similar reason.

Storminess east of the Rockies reached its highest frequency during the last half of February. Essentially, there were two major storm tracks—one along the Canadian border, the other from the Southwest to the Northeast. Both tracks can be reasonably "fitted" to the flow at 700 mb. and to the mean sea level chart. Along the sea level track, associated with the new trough in the Plains, was found the most intense storm of the winter season in the East, as well as those systems responsible for record-breaking precipitation in the Southeast.

REFERENCES

1. R. H. Gelhard, "The Weather and Circulation of December 1960—An Unusually Cold Month in the United States," *Monthly Weather Review*, vol. 89, No. 3, Mar. 1961, pp. 109–114.
2. R. A. Green, "The Weather and Circulation of January 1961," *Monthly Weather Review*, vol. 89, No. 4, Apr. 1961, pp. 137–143.
3. D. E. Martin and W. G. Leight, "Objective Temperature Estimates from Mean Circulation Patterns," *Monthly Weather Review*, vol. 77, No. 10, Oct. 1949, pp. 275–283.
4. W. H. Klein, B. M. Lewis, and I. Enger, "Objective Prediction of Five-Day Mean Temperatures During Winter," *Journal of Meteorology*, vol. 16, No. 6, Dec. 1959, pp. 672–682.
5. U.S. Weather Bureau, *Weekly Weather and Crop Bulletin, National Summary*, vol. XLVIII, Nos. 6 and 10, Feb. 6, and Mar. 6, 1961.
6. U.S. Weather Bureau, *Climatological Data-National Summary*, vol. 12, No. 2, Feb. 1961, Chart IX.
7. W. H. Klein, "Winter Precipitation as Related to the 700-mb. Circulation," *Bulletin of the American Meteorological Society*, vol. 29, No. 9, Part 1, Nov. 1948, pp. 439–453.

Publications by Weather Bureau Authors

S. G. Bigler and P. L. Hexter, Jr., "Radar Analysis of Hurricane Debra," *Proceedings of the Eighth Weather Radar Conference*, San Francisco, 1960, pp. 25–32.

E. W. Burt, "Climatic Digest for Greater Tulsa," The Robert A. Taft Sanitary Engineering Center, *Technical Report* A58–3, Public Health Service, 1958.

K. R. Clark (with E. M. Frisby), "A South Dakota Hail Study, 1954–1959," *Proceedings of the Eighth Weather Radar Conference*, San Francisco, 1960, pp. 143–150.

E. Flowers, "The Atmosphere from the Surface to 50 mb. Over the South Pole, During 1957," pp. 453–462 of *Antarctic Meteorology, Proceedings of the Symposium Held at Melbourne, February 1959*, published for Commonwealth of Australia, Bureau of Meteorology, by Pergamon Press, London, 1960.

T. I. Gray, Jr., "Report of IGY Weather Central 1958," pp. 75–78 of *Antarctic Meteorology, Proceedings of the Symposium Held at Melbourne, February 1959*, published for Commonwealth of Australia, Bureau of Meteorology, by Pergamon Press, London, 1960.

K. J. Hanson, "A Case Study of the Explosive Stratospheric Warming Over the Antarctic, October 1958," pp. 128–137 of *Antarctic Meteorology, Proceedings of the Symposium Held at Melbourne, February 1959*, published for Commonwealth of Australia, Bureau of Meteorology, by Pergamon Press, London, 1960.

G. C. Holzworth (with J. G. Edinger), "Angel Observations With the AN/TPQ–6 at Santa Monica, Calif.," *Proceedings of the Eighth Weather Radar Conference*, San Francisco, 1960, pp. 135–142.

L. F. Hubert, "A Subtropical Convergence Line of the South Pacific—A Case Study Using Meteorological Satellite Data," *Journal of Geophysical Research*, vol. 66, No. 3, Mar. 1961, pp. 797–812.

W. H. Klein, "The Circulation and Weather of 1960," *Weatherwise* vol. 14, No. 1, Feb. 1961, pp. 9–15.

W. H. Klein, B. M. Lewis, C. W. Crockett, and I. Enger, "Application of Numerical Prognostic Heights to Surface Temperature Forecasts," *Tellus*, vol. 12, No. 4, Nov. 1960, pp. 378–391.

J. Korshover, "Synoptic Climatology of Stagnating Anticyclones East of the Rocky Mountains in the United States for the Period 1936–1956," The Robert A. Taft Sanitary Engineering Center, *Technical Report* A60–7, Public Health Service, 1960.

N. Kronberg and J. C. Purvis, "Distribution of Precipitation in South Carolina," *Climatic Series No. 6*, Dept. of Agronomy and Soils, South Carolina Agricultural Experiment Station, Clemson Agricultural College, 1961, 54 pp.

N. Kronberg and J. C. Purvis, "Weather and Corn Production in South Carolina," *Climatic Series No. 5*, Dept. of Agronomy and Soils, South Carolina Agricultural Experiment Station, Clemson Agricultural College, 1960, 25 pp.

D. W. Krueger (with A. A. Foster), "Protection of Pine Seed Orchards and Nurseries from Fusiform Rust by Timing Ferbam Sprays to Coincide With Infection Periods," *Georgia Forest Research Paper No. 1*, Georgia Forest Research Council, Macon, Mar. 1961, 4 pp.

E. H. Markee, Jr., "Effects of Vertical Temperature Difference on Soiling Index," *Air Pollution Control Association Journal*, vol 11, No. 3, Mar. 1961.

E. H. Markee, Jr., "Relationships of an Air Quality Measurement to Meteorological Parameters," *Journal of American Industrial Hygiene Association*, vol. 20, Feb. 1959, pp. 50–55.

P. L. Moore, "The Hurricane Season of 1960," *Weatherwise*, vol. 14, No. 1, Feb. 1961, pp. 18–23.

W. B. Moreland, "Antarctic Stratospheric Circulation and Ozone Observations," pp. 394–409 of *Antarctic Meteorology, Proceedings of the Symposium Held at Melbourne, February 1959*, published for Commonwealth of Australia, Bureau of Meteorology, by Pergamon Press, London, 1960.

K. R. Peterson, "A Precipitable Water Nomogram," *Bulletin of the American Meteorological Society*, vol. 42, No. 2, Feb. 1961, pp. 119–121.

F. W. Reichelderfer, "Meteorological Satellite Systems in Weather Research and Services," *Aerospace Engineering*, vol. 20, No. 3, Mar. 1961, pp. 22–23, 91–97.

F. W. Reichelderfer, "Using Weather Services in Your Business," *Small Marketers Aids*, No. 61, Small Business Administration, Feb. 1961.

V. D. Rockney, "The Radar Program of the U.S. Weather Bureau," *Proceedings of the Eighth Weather Radar Conference*, San Francisco, 1960, pp. 371–376.

M. J. Rubin, "Advection Across the Antarctic Boundary," pp. 378–393 of *Antarctic Meteorology, Proceedings of the Symposium Held at Melbourne, February 1959*, published for Commonwealth of Australia, Bureau of Meteorology, by Pergamon Press, London, 1960.

R. D. Tarble," The Use of Multiple Exposure Radar Photographs in the Weather Bureau's Hydrologic Program," *Proceedings of the Eighth Weather Radar Conference*, San Francisco, 1960, pp. 437–443.

R. C. Taylor, "Mean Monthly Meridional Cross-Sections of Temperature from the South Pole to the North Pole Near 170° E.—A Preliminary Note," pp. 439–452 of *Antarctic Meteorology, Proceedings of the Symposium Held at Melbourne, February 1959*, published for Commonwealth of Australia, Bureau of Meteorology, by Pergamon Press, London, 1960.

L. E. Truppi, "Reduction of Radarscope Data to Digital Form," *Proceedings of the Eighth Weather Radar Conference*, San Francisco, 1960, pp. 459–465.

F. Wells, "An Example of the Use of Radar as an Aid to Local Forecasting Along Coastal Areas," *Proceedings of the Eighth Weather Radar Conference*, San Francisco, 1960, pp. 471–478.

H. Wexler, "Seasonal and Other Temperature Changes in the Antarctic Atmosphere," p. 463 (abstract only) of *Antarctic Meteorology, Proceedings of the Symposium Held at Melbourne, February 1959*, published for Commonwealth of Australia, Bureau of Meteorology, by Pergamon Press, London, 1960.

J. R. Zimmerman, "Wilkes Climatology," pp. 415–422 of *Antarctic Meteorology, Proceedings of the Symposium Held at Melbourne, February 1959*, published for Commonwealth of Australia, Bureau of Meteorology, by Pergamon Press, London, 1960.

New Weather Bureau Publication

Technical Paper No. 39, "Verification of the Weather Bureau's 30-Day Outlooks," by Extended Forecast Section, U.S. Weather Bureau, Washington, D.C., 1961, 58 pp. For sale by Superintendent of Documents, U.S. Government Printing Office, Washington 25, D.C. Price: 40 cents.

Consists of 48 sets of matching forecast and observed charts of 30-day average temperature, precipitation, and 700-mb. pattern for a period of 2 years, preceded by a short discussion of verification statistics covering 6 years and some illustrative examples of use and reliability of the Outlooks.

Recent Articles in Other Weather Bureau Periodicals

Mariners Weather Log, vol. 5

No. 2, March 1961:

"Sea Clutter, a Useful Nuisance," by L. E. Truppi, pp. 31–34.

"Tropical Cyclones in the Eastern North Pacific, 1960," by M. W. Mull, pp. 34–36.

No. 3, May 1961:

"Ice Conditions on the Hudson River, Winter 1960–1961," by J. K. McGuire and W. J. McKee, pp. 65–67.

"Typhoons of the Western North Pacific, 1960," from report of Fleet Weather Central, Guam, pp. 67–76.

U.S. GOVERNMENT PRINTING OFFICE: 1961